HHS Public Access

Author manuscript

Brain Behav Immun. Author manuscript; available in PMC 2020 November 02.

Published in final edited form as:

Brain Behav Immun. 2020 July ; 87: 286–300. doi:10.1016/j.bbi.2019.12.014.

A silent agonist of α7 nicotinic acetylcholine receptors modulates inflammation ex vivo and attenuates EAE

Jean-Rémi Godin[a], **Patrick Roy**[a], **Marta Quadri**[b,c], **Deniz Bagdas**[d], **Wisam Toma**[d], **Ramya Narendrula-Kotha**[e], **Osama A. Kishta**[e], **M. Imad Damaj**[d], **Nicole A. Horenstein**[b], **Roger L. Papke**[c], **Alain R. Simard**[a,e,f,g,*]

[a]Département de Chimie et Biochimie, Université de Moncton, Moncton, NB, Canada

[b]Department of Pharmacology and Therapeutics, University of Florida, PO Box 100267, Gainesville, FL, USA

[c]Department of Chemistry, University of Florida, PO Box 117200, Gainesville, FL, USA

[d]Department of Pharmacology and Toxicology, Medical College of Virginia, Virginia Commonwealth University, Richmond, VA, USA

[e]Northern Ontario School of Medicine, Sudbury, ON, Canada

[f]Department of Chemistry and Biochemistry, Laurentian University, Sudbury, ON, Canada

[g]Department of Biology, Laurentian University, Sudbury, ON, Canada

Abstract

Nicotinic acetylcholine receptors (nAChRs) are best known to function as ligand-gated ion channels in the nervous system. However, recent evidence suggests that nicotine modulates inflammation by desensitizing non-neuronal nAChRs, rather than by inducing channel opening. Silent agonists are molecules that selectively induce the desensitized state of nAChRs while producing little or no channel opening. A silent agonist of α7 nAChRs has recently been shown to reduce inflammation in an animal model of inflammatory pain. The objective of this study was to determine whether a silent agonist of α7 nAChRs can also effectively modulate inflammation and disease manifestation in an animal model of multiple sclerosis. We first evaluated the effects of various nAChR ligands and of an α7 nAChR-selective silent agonist, 1-ethyl-4-(3-(bromo)phenyl)piperazine (m-bromo PEP), on the modulation of mouse bone marrow-derived monocyte/macrophage (BMDM) numbers, phenotype and cytokine production. The non-competitive antagonist mecamylamine and the silent agonist m-bromo PEP reduced

*Corresponding author at: Northern Ontario School of Medicine, 935 Ramsey Lake Rd., Sudbury, ON P3E 2C6, Canada. asimard@nosm.ca (A.R. Simard).

Author contributions

Participated in research design: Simard, Godin, Roy

Conducted experiments: Godin, Roy, Simard, Quadri, Bagdas, Toma, Kishta

Contributed reagents or analytic tools: Simard, Quadri, Horenstein

Performed data analysis: Godin, Roy, Simard, Quadri, Bagdas, Toma, Narendrula-Kotha, Kishta, Damaj, Papke

Wrote or contributed to the writing of the manuscript: Simard, Godin, Quadri, Narendrula-Kotha, Damaj, Horenstein, Papke

Appendix A. Supplementary data

Supplementary data to this article can be found online at https://doi.org/10.1016/j.bbi.2019.12.014.

pro-inflammatory BMDM numbers by affecting their viability and proliferation. Both molecules also significantly reduced cytokine production by mouse BMDMs and significantly ameliorated disease in experimental autoimmune encephalomyelitis. Finally, m-bromo PEP also reduced chronic inflammatory pain in mice. Taken together, our results further support the hypothesis that nAChRs may modulate inflammation via receptor desensitization rather than channel opening. α7 nAChR-selective silent agonists may thus be a novel source of anti-inflammatory compounds that could be used for the treatment of inflammatory disorders.

Keywords

Nicotinic acetylcholine receptors; Silent agonism; Inflammation; Experimental autoimmune encephalomyelitis; Inflammatory pain; Cytokines; CNS inflammation

1. Introduction

It is increasingly clear that nicotinic acetylcholine receptors (nAChRs) play an important role in immune regulation. Multiple studies in mice have shown that nicotine can ameliorate inflammatory diseases such as inflammatory pain [1] and experimental autoimmune encephalomyelitis (EAE) [2–6], a mouse model for multiple sclerosis (MS). Nicotine also inhibits the inflammatory response of human cells [7–11], and although smoking is a risk factor for multiple inflammatory diseases such as MS [12], exposure to nicotine outside of a smoking context is associated with a reduced risk of developing the disease [13]. Altogether, these data support a role for nAChRs in the regulation of the immune response and provides potential therapeutic avenues for treatment of inflammatory diseases.

nAChRs are members of a diverse family of ligand-gated ion channels that are targets for the natural neurotransmitter, acetylcholine [14]. Subunit composition defines each nAChR subtype and dictates their specific and unique biophysical and pharmacological properties. For instance, homomeric α7 nAChRs are much more Ca^{2+}-permeable, are less sensitive to nicotine and desensitize more quickly than heteromeric nAChRs [15,16]. Many studies show that the α7 nAChR is the key subtype involved in nAChR-mediated immune regulation [2,5,6,17–19]. In addition, α7 nAChR-dependent regulation of cytokine production has been shown in multiple immune cell types, including lymphocytes [20], monocytes [9], macrophages [17,21,22], and natural killer cells [23]. The unique physiological, functional and pharmacological characteristics of the α7 nAChR subtype make these receptors prime candidates as drug targets.

The canonical signaling mechanism of nAChRs involves the binding of a standard nAChR agonist, such as acetylcholine or nicotine, which induces a transient opening of the ion channel followed by a period of desensitization [24]. However, α7 nAChRs have a very low probability of opening, even under the most optimized conditions [25]. Additionally, α7 receptors desensitize very rapidly and for prolonged periods in the presence of high agonist concentrations. Such doses of nicotine are necessary to observe anti-inflammatory effects in animal models. It is thus hypothesized that metabotropic signaling activity is induced while the α7 nAChR is in a ligand-bound, non-conducting state [25]. Recently, attention has been drawn to a new class of drugs, termed silent agonists [25–29], which produce very little

channel activation (have < 10% efficacy compared to ACh) but are profoundly desensitizing [27]. Indeed, two silent agonists have been shown to be very effective with in vivo models of neuropathic and inflammatory pain [27,30], supporting the idea that the desensitized state is responsible for the anti-inflammatory roles of the α7 nAChR.

Inflammation and demyelination are hallmark features of MS. Although T cells are thought to drive the immune response in MS and its animal model, experimental autoimmune encephalomyelitis (EAE), the importance of myeloid cells (monocytes, macrophages, microglia, myeloid dendritic cells and neutrophils) in disease pathogenicity is becoming increasingly clear [31]. Myeloid cells are the predominant cells found in active MS brain lesions [32–34], which includes large numbers of monocytes and macrophages. Monocytes and macrophages can contribute to disease progression by promoting inflammation but also have a role in repair mechanisms crucial to disease recovery [32]. These contrasting roles can be explained by the spectrum of monocyte and macrophage cell phenotypes. Recent trends have been to classify these cells into two major populations: classically-activated and alternatively-activated monocytes/macrophages, respectively referred to as M1 and M2 cells [35]. It is generally accepted that M1 cells primarily contribute to the inflammatory response, while M2 cells play important roles in the resolution of immune responses and recovery [36–38]. In reality however, monocyte and macrophage populations consist of cells that exist in a spectrum between these two extremes [39]. A shift in the balance towards either M1 or M2 can therefore indicate the overall nature of the inflammatory response.

Murine M1 cells are generally accepted to be positive for CCR2 and express high levels of Ly6C (thus often called $CCR2^{+}Ly6C^{high}$ cells), while CD80, CD86 and MHC-II are generally up-regulated [35,40,41]. They can also be characterized by their significant production of the cytokines TNF-α, IL-1β, IL-6 and IL-12 and their ability to induce the differentiation of pro-inflammatory Th1 T cells [35,41,42]. These cells are predominantly produced and recruited to tissues under inflammatory conditions [42], such as the CNS in MS and EAE [5,32,43,44], and contribute significantly to disease pathology. On the other hand, M2 cells express CX3CR1, little or no CCR2, and lack Ly6C [35,40,41]. Other commonly-used markers for M2 cells are CD206 (Mannose receptor) and Arginase 1 (Arg1), although not all M2 cells express these proteins, and Arg1 can also be found in M1 cells in certain conditions [39]. These cells instead produce IL-10 and TGF-β more abundantly and preferentially mediate the differentiation of anti-inflammatory Th2 T cells [35,40,41]. Interestingly, M2 cells have been shown to increase the differentiation of regulatory T cells and to have beneficial effects in EAE [37,38]. The balance between M1 and M2 cells in MS and EAE, and by extension the beneficial and detrimental consequences of immune activity, depend on endogenous mechanisms that regulate immune cell functions.

We and others have shown that administration of nicotine attenuates the severity of symptoms in EAE, mainly via the α7 nAChR [2–6]. These studies also demonstrated that nicotine inhibits leukocyte entry into the CNS of EAE mice and shifts the cytokine secretion profile away from the M1/Th1/Th17 response. In light of the recent publications demonstrating that α7 nAChR silent agonists reduce inflammatory pain [27,30], the goal of the present study was to test the hypothesis that a silent agonist of the α7 nAChR would reduce bone marrow-derived monocyte/macrophage (BMDM) numbers and protect against

EAE. Using a variety of α7 nAChR-selective and non-selective ligands, such as agonists, antagonists, as well as a α7-selective silent agonist 1-ethyl-4-(3-(bromo)phenyl)piperazine (m-bromo PEP) [29], we first provide evidence that α7 nAChR-dependent effects on BMDM numbers, phenotype and cytokine production ex vivo are likely due to non-conducting channel conformations. We then confirm our findings in vivo, by showing that both mecamylamine and m-bromo PEP significantly delay the onset and reduce the severity of EAE, while lowering the numbers of pro-inflammatory cells in the CNS in conjunction with altered chemokine, integrin and metalloprotease expression within the brain. Finally, we confirm previous studies showing that α7 nAChR silent agonism also reduces inflammatory pain [27,30]. Taken together, our results support the hypothesis that silent agonists of α7 nAChRs modulate pro-inflammatory responses, likely by inducing a non-conductive receptor state rather than via channel opening.

2. Methods

2.1. Animals

2.1.1. Bone marrow cultures and EAE—C57BL/6J mice (stock number 000664) were purchased from The Jackson Laboratory (Bar Harbor, MA, USA). All animals were housed in individually micro-ventilated cages, up to 5 mice per cage, in a 21 °C humidity-controlled animal facility. The rooms were on a 12-hour light/dark cycle (lights on at 7:00 AM). All experiments were performed during the light cycle (between 7:00 AM and 7:00 PM). Animals were in good health at the time of experimentation. Mice used were at least 7–8 weeks of age at the experiment's inception. For bone marrow collection and EAE experiments not requiring brain collection, euthanasia was performed by anesthetizing mice with isoflurane followed by cervical dislocation. For EAE experiments requiring brain collection, mice were anesthetized by isoflurane, and euthanized by cardiac perfusion with phosphate-buffered saline (PBS). The experiments were reviewed, approved and conducted in accordance with the policies outlined by the Canadian Council for Animal Care and were approved by the Université de Moncton (protocol #13–02) and Laurentian University (protocol #2017–08–01) animal care committees.

2.1.2. Inflammatory pain experiments—Male adult (8–10 weeks of age) Institute of Cancer Research (ICR) mice were obtained from Harlan Laboratories (Indianapolis, IN). Mice were housed in a 21 °C humidity-controlled animal care facility approved by the Association for Assessment and Accreditation of Laboratory Animal Care. They were housed in groups of four and had free access to food and water. The rooms were on a 12-hour light/dark cycle (lights on at 7:00 AM). All experiments were performed during the light cycle (between 7:00 AM and 7:00 PM), and the study was approved by the Institutional Animal Care and Use Committee of Virginia Commonwealth University (protocol #AM10142). All studies were carried out in accordance with the National Institutes of Health's Guide for the Care and Use of Laboratory Animals. Animals were sacrificed via CO_2 followed by cervical dislocation after the experiments were finished, unless noted otherwise. Any subjects that subsequently showed behavioral disturbances unrelated to the pain induction procedure were excluded from further behavioral testing.

2.2. Chemicals

1-ethyl-4-(3-(bromo)phenyl)piperazine (m-bromo PEP; See Suppl. Fig. 1) was synthesized as described previously [29]. PNU-120596 was synthesized following the published procedure [45]. Fresh acetylcholine (ACh; Sigma-Aldrich, Saint-Louis, MO, USA) stock solutions were made each day of experimentation. PNU-120596 and m-bromo PEP stock solutions were prepared in dimethylsulfoxide (DMSO) (Sigma-Aldrich) and stored at −20 °C. Nicotine bitartrate (Sigma-Aldrich), mecamylamine (Tocris Bioscience, Bristol, UK), α-bungarotoxin (αBgt; Tocris), AR-R17779 (Tocris), recombinant human M-CSF (Sigma-Aldrich) and IFNγ (Cell Guidance Systems, Cambridge, UK) were prepared in PBS, stored at −20 °C. All working drug solutions were prepared fresh each day at the desired concentration from the stored stock. All doses are expressed as the free base of the drug.

2.3. Heterologous expression of nAChRs in Xenopus laevis oocytes

Xenopus laevis oocytes were injected with human α7 nAChR clones obtained from Dr. Jon M. Lindstrom (University of Pennsylvania, Philadelphia, PA) to heterologously express α7 nAChRs. To improve the level and speed of α7 subtype expression without affecting its pharmacological properties [46], the human RIC3 clone was coinjected with α7. RIC3 was obtained from Dr. Millet Treinin (Hebrew University, Jerusalem, Israel). Before the injection, plasmid cDNAs were first linearized and purified, and then RNAs were prepared using the mMessage mMachine in vitro RNA transcription kit (Ambion, Austin, TX). Oocytes were surgically removed from mature *Xenopus laevis* frogs (Nasco, Ft. Atkinson, WI) and subsequently injected with appropriate nAChR subunit RNAs as described previously [47]. Frogs were maintained in the Animal Care Service facility at the University of Florida, and all procedures were approved by the University of Florida Institutional Animal Care and Use Committee. All studies were carried out in accordance with the National Institutes of Health's Guide for the Care and Use of Laboratory Animals. Briefly, the frog was first anesthetized for 15–20 min in 1.5 L frog tank water containing 1 g of 3-aminobenzoate methanesulfonate buffered with sodium bicarbonate. The harvested oocytes were treated with 1.25 mg/ml collagenase (Worthington Bio-chemicals, Freehold, NJ) for 2 h at room temperature (RT) in a calcium-free Barth's solution (88 mM NaCl, 1 mM KCl, 2.38 mM $NaHCO_3$, 0.82 mM $MgSO_4$, 15 mM HEPES, and 12 mg/l tetracycline, pH 7.6) to remove the follicular layer. Stage V oocytes were subsequently isolated and injected with 50 nl of 5–20 ng nAChR subunit RNA. Recordings were carried out 1–7 days after injection.

2.4. Two-electrode voltage-clamp electrophysiology

Experiments were conducted using OpusXpress 6000A (Molecular Devices, Union City, CA). The OpusXpress recording system has previously been described in detail [47]. In brief, OpusXpress provides two-electrode voltage clamp of eight oocytes in parallel, including steady bath perfusion, drug delivery, and data acquisition. Both the voltage and current electrodes were filled with 3 M KCl. Oocytes were voltage clamped at −60 mV at RT (24 °C). The oocytes were bath perfused with Ringer's solution (115 mM NaCl, 2.5 mM KCl, 1.8 mM $CaCl_2$, 10 mM HEPES, and 1 mM atropine, pH 7.2) at 2 ml/min. To evaluate the effects of experimental compound compared with ACh-evoked responses

of various nAChR subtypes expressed in oocytes, baseline control ACh responses were defined by two initial applications of ACh made before test applications of experimental compound. The agonist solutions were applied from a 96-well plate via disposable tips, and the test compound was applied alone or co-applied with PNU-120596. Drug applications were 12 sec in duration followed by a 181 sec washout period. A typical recording for each oocyte constituted two initial control applications of ACh, an experimental compound application, and then a follow-up control application of ACh to determine the desensitization or possible rundown of the receptors. The control ACh concentration was 60 μM for α7 nAChR experiments. The responses were measured as net charge amplitudes for the α7 data, as previously described [48]. Data were collected at 50 Hz, filtered at 20 Hz, analyzed by Clampfit 9.2 (Molecular Devices) and Excel 2003 (Microsoft, Redmond, WA), and normalized to the averaged net charge response of the two initial ACh controls [48]. Data were expressed as mean ± SEM from at least four oocytes for each experiment and plotted by KaleidaGraph 4.5.2 (Abelbeck Software, Reading, PA). Receptor-mediated activity has a limit of detection of approximately 0.05% of the ACh controls.

2.5. Bone marrow collection

Naive mice were anesthetized with isoflurane and euthanized by cervical dislocation. Femurs and tibias were collected and cleaned from each mouse. Bones were sterilized in 70% EtOH (Sigma-Aldrich) for 2 min before bone marrow (BM) was collected by flushing out of the bone with sterile PBS. Clumps were broken down and cells were pelleted at 300×*g* for 15 min. Cells were resuspended in 5 ml of red blood cell (RBC) lysis buffer (BioLegend, Pacific Heights, CA, USA) to remove RBCs. Lysis was stopped after 5 min, and cells were strained through a 40 μm filter. Cells were then counted and centrifuged at 450 × g for 5 min. They were counted using a Moxi^2 Mini Automated Cell Counter (Orflo Technologies, Ketchum, ID, USA) and resuspended at a final concentration of 2×10^6 cells/ml in RPMI 1640 medium containing 2 mM L-glutamine (Sigma-Aldrich) supplemented with 10% Heat-inactivated fetal bovine serum (FBS) (HI-FBS; Wisent Bioproducts, St-Bruno, QC, Canada) and 5% pen/strep (Wisent Bioproducts).

2.6. Mouse bone marrow derived monocytes/macrophages (BMDMs)

After bone marrow collection and preparation, 30 ng/ml recombinant human M-CSF (Sigma) and 20 ng/ml recombinant murine IFNγ (Sigma) were added to the culture media, and cells were incubated for 72 h (37 °C, 5% CO_2) for monocyte and macrophage differentiation and polarization. Nicotine, αBgt, mecamylamine, AR-R17779 or m-bromo PEP were added to the culture medium as indicated. The concentrations for each drug treatment are indicated in the relevant results section and figure legend. All control culture conditions for m-bromo PEP were supplemented with 0.1% DMSO (Sigma-Aldrich) to control for the treatment's vehicle. Cells were cultured for 72 h. Suspended cells were harvested by gentle pipetting of the medium, and adherent cells were washed with PBS and detached using a 10 mM EDTA solution at a pH of 7.4. Suspension (including monocytes) and adherent (including macrophages) cells were combined and pelleted at 450×*g* for 5 min at RT. The supernatant was removed, and cells were washed once by adding 10 ml of PBS followed by a 5 min spin at 450×*g*. After the wash, cells were resuspended in PBS at a concentration of 1×10^6 cells/100 μl. Cells were then used for flow cytometry.

2.7. Cytokine measurements

Bone marrow was collected and BMDMs cultured as described before, but only for 48 h. Cells were then stimulated with 100 ng/ml LPS (Sigma-Aldrich) for 6 h. Cells were treated with mecamylamine, m-bromo PEP or vehicle (PBS or 0.1% DMSO, respectively) throughout the 48 h culture and 6 h stimulation. Supernatant was subsequently collected, and cytokine concentrations were assessed using LEGENDplex kits for TNFα, IL-1β, IL-6, IL-12 and IL-10 (BioLegend), as per the manufacturer's instructions. Bead fluorescence was measured by flow cytometry using a CytoFLEX (Beckman Coulter, Pasadena, CA, USA), and analyzed using the LEGENDplex™ Data Analysis Software (BioLegend).

2.8. In vivo drug treatment for EAE experiments

Osmotic pumps, model 2002 (Alzet, DurectCorporation, Cupertino, CA, USA), were inserted subcutaneously on the back of mice 24 h before the induction of EAE and used to deliver mecamylamine or m-bromo PEP at a mean rate of 0.5 μl per hour. Doses were calculated to be 6.5 mg/kg/day (in PBS) for mecamylamine and 6 mg/kg/day (in 5% DMSO) for m-bromo PEP. Previous studies showed that delivery of 50% DMSO over 14 days using the same pump model [49], or 5% DMSO sub-cutaneous injection (50 μl volume) [50] had no effect on EAE severity or disease onset. Due to an uncontrollable shortage of osmotic pumps, control mice received a sham pump-implantation surgery. On Day 16 post immunization, pumps were removed from drug-treated EAE mice. For all surgeries, mice were anesthetized with isoflurane, given 0.1 mg/kg (i.p.) of buprenorphine 20 min prior to surgery.

2.9. Induction of EAE

On day 0, C56BL/6 mice received a subcutaneous injection in both rear flanks containing 200 μg of MOG35–55 peptide (MOG) (Amino acid sequence: M-E-V-G-W-Y-R-S-P-F-S-R-VV-H-L-Y-R-N-G-K; Synpeptide, Shanghai, CHN) and Complete Freund's adjuvant (CFA) (Difco, Detroit, MI, USA), which contains 500 μg of desiccated non-viable *M. Turberculosis* (Difco, Detroit, MI, USA). Simultaneously, they received an intraperitoneal injection of 200 ng of *Pertussis Toxin* (PT) (List Biologic, Campbell, CA, USA). Mice received a second dose of PT two days later.

2.10. EAE clinical scores were evaluated as follows

Scores were attributed every day in 0.5 increments by the same person, blind to treatment groups, for the duration of the time course. Score weights were as followed: 0.5 = weakness in the tail; 1.0 = Limp tail; 1.5 = Limp tail and weakness of 1 hind leg; 2.0 = Limp tail and weakness of hind legs; 2.5 = Limp tail and dragging hind legs; 3 = Limp tail and complete paralysis of hind legs; 3.5 = Limp tail and hind leg paralysis, unable to turn over when flipped on its side; 4.0 = Limp tail, complete hind leg and partial front leg paralysis; 4.5 = Limp tail, complete hind leg paralysis, partial front leg paralysis, no longer responds to stimuli; 5.0 = Moribund or deceased. Mice that reached a score of 4.0 for two consecutive days or a score of 5 were immediately euthanized. Mice that showed signs of dehydration were injected with 0.25 ml of Normosol-R, three times per day at three different subcutaneous injection sites.

2.11. Brain tissue collection from EAE mice

EAE mice were sacrificed at peak inflammation (13 or 16 days post immunization). Immune cells were removed from the brain's vasculature by intra-cardiac perfusion with ice-cold PBS. Mouse brains were collected immediately afterwards. Brains were then subjected to enzymatic digestion using the Tumor Dissociation Kit II (Miltenyi Biotec, Auburn, CA, USA) and dissociated using the gentleMACS™ Octo Dissociator with Heaters (Miltenyi Biotec), using the default program for tumor tissue, and in accordance with the manufacturer's directives. Cells were pelleted at 300×*g* for 10 min at RT and strained through a 70 μm filter to remove myelin and aggregates. They were pelleted again at 300×*g* for 10 min and further myelin removal was achieved by re-suspending cells in 2 ml of 0.9 M sucrose (AMRESCO) and doing a further centrifugation at 700×*g* for 15 min at RT. Supernatant was discarded, and cells were washed with PBS, followed by a spin at 450×*g* for 5 min at RT. Cells were resuspended in 2 ml PBS, split in half, and prepared for flow cytometry or RNA extraction.

2.12. Flow cytometry

Experiments involving flow cytometric analysis of cell numbers and phenotype were performed with a MoFlo™ XDP High-Performance Cell Sorter (Beckman Coulter) or a FC500 cytometer (Beckman Coulter). Single cell suspensions from the various tissues were resuspended at the concentration of 10^5-10^6 cells/100 μl. Fc receptors were blocked prior to staining with TruStain fcX (BioLegend). Cells were analyzed by staining for one or more of the following mouse antigens (targeted by the indicated antibody fluorescently tagged with either FITC, Alexa Fluor 488, PE, Pacific Blue, Brilliant Violet 570, APC, Alexa Fluor 700, APC/Cy7 or PE/Cy7): CD3, Ly-6G, CD19, CD11b, CD45, CCR2, Ly-6C, CD206, CD80, CD86 and MHC-II. Antibodies were purchased from BioLegend except for CCR2, which was purchased from R&D Systems (Burlington, ON, Canada). Appropriate isotype controls were included. Cell viability was determined using the 7-AAD marker (BioLegend). Cell proliferation was assessed with eFluor 670 (ThermoFisher). Results were analyzed using the software Kaluza, version 2.1 (Beckman Coulter). For ex vivo experiments, BMDMs were identified as $CD11b^+CD45^+Ly6G^-$ and neutrophils as $CD11b^+CD45^+Ly6G^+$. For in vivo experiments, gating strategy to identify cell types in the brain was as follows: leukocytes ($CD45^+$), T cells ($CD3^+CD45^+$), B cells ($CD19^+CD45^+CD3^-$), neutrophils ($CD11b^+CD45^+Ly6G^+$), infiltrating monocytes ($CD11b^+CD45^{high}Ly6G^-$) and microglia ($CD11b^+CD45^{low}Ly6G^-$).

2.13. Quantitative real time PCR (qRT-PCR)

Cells were lyzed in RiboZol (Amresco, Solon, OH, USA) and frozen at −80 °C until future use. RNA was then purified using RNeasy purification kit (Qiagen, Valencia, CA, USA). Reverse transcription was achieved with qScript XLT cDNA SuperMix (Quantabio, Beverly, MA, USA) as per the supplied protocol, followed by RNA digestion with RNAse H (2 U/μl) at 37 °C for 20 min (Ambion, Burlington, ON, Canada). qRT-PCR was done with SsoAdvanced SYBRGreen Supermix (Bio-Rad, Hercules, CA, USA). GAPDH and ACTB were used as reference genes for normalization. The following primer sequences (Integrated DNA Technologies, Inc., Coralville, Iowa, USA) were used for mRNA expression analysis:

Gene	Forward Primer	Reverse Primer
CCL2	5′-CTGCTGTTCACAGTTGCCG-3′	5′-GCACAGACCTCTCTCrTGAGC-3′
CX3CL1	5′-CACGAATCCCAGTGGCTTTG-3′	5′-GGCGTCTTGGACCCATTTCT-3′
CXCL1	5′-TGGCTGGGATTCACCTCAAG-3′	5′-CCGTTACTTGGGGACACCTT-3′
CXCL2	5′-AGGGCGGTCAAAAAGTTTGC-3′	5′-CAGGTACGATCCAGGCTTCC-3′
CCL19	5′-CCTGGGAACATCGTGAAAG-3′	5′-AGCCCCTTAGTGTGGTGAACAC-3′
CCL21	5′-ATCCCGGCAATCCTGTTCTC-3′	5′-GGTTCTGCACCCAGCCTTC-3′
MMP-9	5′-TAGATCATTCCAGCGTGCCG-3′	5′-GCCTTGGGTCAGGCrTAGAG-3′
VCAM	5′-TGAACCCAAACAGAGGCAGAGT-3′	5′-GGTATCCCATCACTTGAGCAGG-3′
ICAM	5′-CAATTTCTCATGCCGCACAG-3′	5′-AGCTGGAAGATCGAAAGTCCG-3′
GAPDH	5′-AGCCTCGTCCCGTAGACAA-3′	5′-ATGAAGGGGTCGTTGATGGC-3′
ACTB	5′-GGCTGTATTCCCCTCCATCG-3′	5′-CAGTTGGTAACAATGCCATGT-3′

Cycle condition were 95 °C for 30 sec, followed by 40 cycles of 95 °C for 5 sec and 60 °C for 30 sec, finally a melt curve 65–95 °C (0.5 °C increment) for 5 sec/step. Results were analyzed using CFX manager™ software version 3.1. No template and no reverse-transcriptase controls were always included in each reaction. Melt curve analysis and gel electrophoresis confirmed the presence of only one band with the expected transcript length.

2.14. Monocyte migration assay

Bone marrow cells were flushed from the femur and tibia of naive mice, as described earlier. Monocytes were isolated using the Mouse Monocyte Isolation Kit (BM) (Miltenyi Biotec, Auburn, CA, USA) as per the supplied protocol. Monocyte purity of > 90% was confirmed by flow cytometry. Cell migration was then evaluated using the InnoCyte™ Monocyte Cell Migration Assay (EMD Millipore Corp., Temecula, CA, USA), as detailed in the supplied protocol. Briefly, 4×10^5 of the enriched monocytes in RPMI 1640 medium containing 5% HI-FBS and 100 μM mBrPEP or 0.1% DMSO were placed in the upper chamber of 5 μm pore size inserts. The lower chamber contained 100 ng/ml CCL2 in RPMI 1640 medium containing 5% HI-FBS, or the medium and HI-FBS without CCL2 for the negative controls. Cells were incubated for 3 h in a CO_2 cell culture incubator. Following the steps described in the migration assay protocol, migrated cells in the lower chamber were then quantified using Calcein-AM, and measured with a FLUOstar Optima (BMG Labtech, Ortenberg, Germany).

2.15. Complete Freund's Adjuvant (CFA)–induced inflammatory pain model

We explored the effects of m-bromo PEP in the CFA test, composed of inactivated and dried *Mycobacterium tuberculosis* (Sigma-Aldrich), a widely used model of persistent inflammatory pain. The CFA model is based on hypersensitivity, paw swelling, and nuclear factor-kB–mediated transcription of tumor necrosis factor α involved in the formation of the principal mediators of inflammation [51]. Mice were injected intraplantarly with 20 μl of CFA (50%, diluted in mineral oil; Sigma-Aldrich). Sham mice were injected with vehicle (mineral oil). Mechanical sensitivity (see the measurement of the von Frey test) was measured before and 3 days after CFA injection. m-bromo PEP (1, 3.3, and 10 mg/kg), dissolved in a mixture of 2:2:16 [2 vol ethanol/2 vol Emulphor-620 (Rhone-Poulenc, Inc.,

Princeton, NJ, USA)/16 volumes distilled water], or vehicle was injected intraperitoneally on day 3 after CFA injection, and mice were tested for mechanical sensitivity at different time points (15, 30, and 60 min) after drug injection. Paw diameter was also measured 1 h after m-bromo PEP (10 mg/kg) or vehicle. The thickness of the CFA treated paws were measured both before and after injections at the time point indicated above, using a digital caliper (Traceable Calipers, Friendswood, TX). Data were recorded to the nearest ± 0.01 mm and expressed as change in paw thickness (ΔPD = difference in the ipsilateral paw diameter before and after injection paw thickness).

2.16. Evaluation of mechanical sensitivity

Mechanical sensitivity thresholds were determined according to the method of [52] and as adapted in [53]. A series of calibrated von Frey filaments (Stoelting, Wood Dale, IL, USA) with logarithmically incremental stiffness ranging from 2.83 to 5.07 expressed as diameter sensitivity (ds) log 10 of 10× force (in milligrams) was applied to the paw with a modified up-down method [54]. The mechanical threshold was expressed as log 10 of 10× force (in milligrams), indicating the force of the von Frey hair to which the animal reacted (paw withdrawn, licking, or shaking). All behavioral testing on animals was performed in a blinded manner.

2.17. Statistical analysis

Statistical analysis was performed using GraphPad Prism 8.2.1 (GraphPad Software, La Jolla, CA, USA). For experiments involving a sample number of 8 or higher (Figs. 2 and 3), normal distribution was tested with the Omnibus K^2 normality. Since no significant deviation from normality was detected, data were analyzed using a repeated-measures one-way ANOVA, followed by a post-hoc multiple comparisons with Dunnett's correction. For experiments with one or more groups with a sample number below 8 (all other figures), data were analyzed using non-parametric statistical tests. This involved either the Friedman repeated-measures one-way ANOVA or Kruskal-Wallis one-way ANOVA, both followed by multiple comparisons with Dunn's correction. Details on statistical test used for each experiment can also be found in the relevant results sections and figure legends.

3. Results

3.1. The non-competitive antagonist mecamylamine reduces BMDM cell numbers

Bone marrow cells were obtained from wild-type (WT) mice and cultured in the presence of M-CSF, IFNγ and various nAChR ligands for 3 days to induce the production and differentiation of BMDMs (Fig. 1A). Neither nicotine or αBgt alone, or in combination, had any significant effect on macrophage cell numbers. Surprisingly however, with a combination treatment of nicotine and mecamylamine, a non-competitive nAChR antagonist thus preventing channel opening while allowing agonist binding, significantly reduced BMDM cell numbers. Mecamylamine alone had a similar effect on the number of BMDMs. Contrarily, the α7 nAChR-selective full agonist AR-R17779 had no effect on BMDM numbers. We then determined if the reduction of BMDM numbers by mecamylamine was dose-dependent (Fig. 1B). Again, nicotine alone only caused a slight reduction in the number of BMDMs, although the effect did not reach statistical significance with only an

sample number of n = 3. However, treating cells with a combination of nicotine plus 10 μM, 33 μM, 66 μM or 100 μM mecamylamine revealed a trend in further reduction, although still not reaching statistical significance. Similar results were obtained with cells treated with increasing doses of mecamylamine in the absence of nicotine. Mecamylamine had no effect on undifferentiated cells. Even though these preliminary experiments were were carried out with small sample numbers, these data nonetheless suggested that mecamylamine regulates BMDM cell numbers via nAChRs through unknown channel-independent mechanisms.

3.2. Mecamylamine and a silent agonist of α7 nAChR reduce proinflammatory BMDM numbers by affecting their viability and proliferation

The α7 nAChR subtype has been shown to be the main contributor of nAChR-dependent anti-inflammatory effects [2,5,6,17–19]. As previously described, mounting evidence suggests that regulation of immune cell responses by α7 nAChRs may occur independently of the ion channel functions of the receptor. In order to test this hypothesis, we made use of m-bromo PEP, a nAChR silent agonist shown to be selective for the α7 nAChR subtype in Xenopus oocytes (Suppl. Fig. 1). As previously reported [29], at 30 μM m-bromo PEP produces virtually no α7 activation in Xenopus oocytes when applied alone but induces large responses in co-application with PNU-120596, a type II positive allosteric modulator selective for the α7 nAChR. To better investigate both its α7 partial agonism and desensitizing properties, we tested m-bromo PEP at a broader range of concentrations (30, 100 and 300 μM), alone and in co-application with PNU-120596 according to the reported protocol [26]. Since the concentration-dependent receptor desensitization prevents the measurement of peak currents at high agonist concentrations [48], we used net charge as the primary measurement of α7 nAChR responses. Despite showing virtually no activation of the α7 receptor subtype at all concentrations tested (< 1% relative to 60 μM ACh control responses), m-bromo PEP promoted greater receptor desensitization with increasing concentrations; this is evidenced by PNU-120596 co-application, with 300 μM m-bromo PEP inducing approximately 10 times deeper desensitization compared to 100 μM. These results highlight a silent agonism profile at all the concentrations tested for m-bromo PEP on the α7 receptor in Xenopus oocytes.

We thus repeated the previous BMDM culture experiment, except cells were treated with mecamylamine (100 μM), m-bromo PEP (100 μM), or vehicle (PBS for mecamylamine and 0.1% DMSO for m-bromo PEP) for 3 days. Cells were then analyzed by flow cytometry to identify BMDMs, and assess their numbers, phenotype, viability and proliferation (Fig. 2). No differences were observed between PBS and 0.1% DMSO controls, and thus only 0.1% DMSO control data are shown. Differentiation with mecamylamine or m-bromo PEP treatments significantly reduced total cell count as compared to the differentiated non-treated group. Similarly, mecamylamine partially negated BMDM numbers, while this effect was more prominent in m-bromo PEP-treated cells. Contrarily, neutrophil abundance was not significantly affected by m-bromo PEP but was significantly reduced by mecamylamine.

We then determined whether the drugs selectively altered the abundance of M1 or M2 cells. Differentiation of BMDMs by M-CSF and IFNγ increased $Ly6C^{high}CCR2^{+}$ M1 BMDM numbers compared to non-differentiated cells. Mecamylamine and m-bromo PEP reduced

M1 cell counts as compared to M-CSF + IFNγ-differentiated cells. However, m-bromo PEP increased the proportions of BMDMs that were CD80^{high}, while mecamylamine had no effect. The proportion of BMDMs that were CD86^{high} or MCH-II^{high} were unchanged by either molecule. Interestingly however, the proportion of BMDMs with high levels of CD206, a surface marker for M2 cells, was significantly increased by m-bromo PEP but not mecamylamine.

To further ascertain the mechanisms by which mecamylamine and m-bromo PEP reduce BMDM numbers, we assessed the effects of these drugs on cell viability and proliferation. We found that mecamylamine and m-bromo PEP modestly reduced cell viability by approximately 5%, and effect that nonetheless reached statistical significance. Similarly, the mean proportion of parent hematopoietic stem cell (HSC)-derived BMDMs that remained after 3 days of culture was increased by m-bromo PEP. The percentage of BMDMs derived from the first generation of HSCs were unchanged by mecamylamine or m-bromo PEP. Mecamylamine also had no effect on the percentage of BMDMs derived from second generation HSCs, while the proportions of these cells were slightly reduced by m-bromo PEP, although the effect did not reach statistical significance. Overall, these data suggest that mecamylamine and m-bromo PEP reduce total and M1 BMDM cell numbers by partially reducing both cell viability and proliferation, and that m-bromo PEP increases the expression of CD206, a M2 cell marker.

3.3. Mecamylamine and m-bromo PEP modulate LPS-induced cytokine expression

We thus investigated whether these two molecules could alter the inflammatory response of BMDMs by measuring the secretion of the pro-inflammatory cytokines TNFα, IL-1β, IL-6, IL-12, and the anti-inflammatory cytokine IL-10 (Fig. 3). To this end, BM cells were cultured with M-CSF and IFNγ to induce the production of M1 BMDMs. After two days of culture, cells were stimulated with 100 ng/mL LPS for 6 h, and cytokines were then measured in the supernatant. Cells were treated with each drug (100 μM) or vehicle (PBS or 0.1% DMSO for mecamylamine and m-bromo PEP, respectively) during both the 48 hr culture period and the 6 hr LPS stimulation. We found that TNFα and IL-10 secretion was reduced by mecamylamine and m-bromo PEP, while IL-6 was only inhibited by m-bromo PEP. IL-1β and IL-12 levels were below detection limits in most samples and are therefore not shown.

3.4. Mecamylamine reduces EAE clinical scores and the numbers of peripherally derived cell numbers in the CNS

Since both mecamylamine and m-bromo PEP influenced CCR2^{+}Ly6C^{high} cell numbers ex vivo, and inhibited the secretion of multiple cytokines, we next evaluated whether both molecules could alter the disease course in EAE mice, starting with mecamylamine (Fig. 4). We found a significant decrease in the clinical scores of mecamylamine-treated EAE (EAE + Meca; 6.5 mg/kg/day) mice, compared EAE mice, for the overall time course. The average peak clinical score was decreased in EAE + Meca compared to EAE, while the days to disease onset was marginally increased. Our previous findings showed that nicotine similarly protects against EAE by reducing pro-inflammatory cell recruitment to the CNS [2,3,5,6]. We therefore assessed immune cells in the brain of EAE + Meca mice compared to EAE

mice at peak disease, which corresponded to 13 days post-immunization in this experiment (also see Suppl. Fig. 2 for disease scores of the 13 day experiment). T lymphocytes ($CD3^+CD45^+$) and B lymphocytes ($CD3^-CD19^+CD45^+$) accounted for a lower proportion of total leukocytes in EAE + Meca compared to EAE, while the effects on neutrophils ($CD11b^+Ly6G^+CD45^+$) did not reach statistical significance. Similarly, the proportion of leukocytes that were identified as infiltrating monocytes ($CD11b^+Ly6G^-CD45^{high}$) were also significantly reduced in EAE + Meca. Of these infiltrating monocytes, the proportion that were M1 cells ($Ly6C^{high}CCR2^+$) were also significantly reduced by mecamylamine. As expected, the increase numbers of infiltrating leukocytes in the CNS of EAE mice caused a relative reduction in the proportion of leukocytes that identified as microglia ($CD11b^+Ly6G^-CD45^{low}$), an effect that was reversed by mecamylamine. Overall, these data demonstrate that mecamylamine treatment reduced the clinical scores and reduced the numbers of peripheral pro-inflammatory immune cells that enter the CNS of EAE mice.

We therefore next assessed whether the reduced numbers of immune cells observed in the CNS of EAE + Meca mice was due to changes in chemokines, metalloproteinases and adhesion molecules (Fig. 5). Mecamylamine reversed the EAE-induced increase in the mRNA expression of CCL2 (recruitment of M1 macrophages), CXCL2 (neutrophils) and CCL19 (T and B lymphocytes), each reaching statistical significance. CXCL1 was marginally reduced, while CCL21 (T lymphocytes) was unaffected by mecamylamine treatment. Mecamylamine significantly inhibited the mRNA expression of the metalloproteinase MMP-9 and the integrin ICAM, while VCAM was unaffected.

3.5. m-bromo PEP reduces EAE clinical scores and the numbers of peripherally-derived cell numbers in the CNS

As shown in Fig. 6, m-bromo PEP (EAE + m-bromo PEP; 6 mg/kg/day) similarly decreased the overall clinical scores compared to EAE mice. The peak clinical scores were lower, while the days to disease onset were higher, in EAE + m-bromo PEP compared to EAE mice. Most m-bromo PEP-treated mice had not displayed any sign of disease at day 13, therefore brain collection was delayed until 16 days post-immunization in this experiment (also see Suppl. Fig. 3 for disease scores). m-bromo PEP reversed the proportions of T cells and B cells in the CNS normally observed in EAE mice. However, the drug did not significantly affect neutrophils. Interestingly, m-bromo PEP also significantly reduced the proportions of infiltrating monocytes, however, the proportion of those monocytes that were M1 cells was unaffected. Nonetheless, due to the reduced numbers of total infiltrating monocytes, the proportion of M1 cells with respect to total leukocytes was significantly lower in EAE + m-bromo PEP compared to EAE mice (data not shown). As expected, the proportions of leukocytes identified as microglia were returned to normal after m-bromo PEP treatment. Overall, these data show that m-bromo PEP effectively reduced the clinical scores and the proportions of pro-inflammatory immune cells in the CNS of EAE mice.

mRNA expression analyses (Fig. 7) revealed that m-bromo PEP prevented the EAE-induced increase in the chemokines CCL2, CXCL2 and CCL19. The drug also induced an increase in the expression of CX3CL1 compared to the EAE group. In addition, m-bromo PEP did not affect MMP-9 and ICAM, while the molecule caused an increase in the expression of

VCAM mRNA. We then tested whether m-bromo PEP could directly modulate the CCL2-induced migration of naïve monocytes using Boyden-chamber migration assays (Suppl. Fig. 4). CCL2 caused an approximately 2-fold increase in cell migration relative to the negative control. This effect was not reversed by 100 μM m-bromo PEP. These data therefore suggest that m-bromo PEP inhibits the influx of pro-inflammatory cells from the periphery into the CNS of EAE by modulating chemokine and integrin expression within the brain.

3.6. m-bromo PEP attenuates CFA-induced inflammatory pain

It was recently shown that p-CF_3 diEPP, another phenylpiperazine-based silent agonist, reduces inflammatory pain [30]. We thus confirmed whether m-bromo PEP would similarly inhibit inflammation in the same animal model for inflammatory pain. As reported in Suppl. Fig. 5, m-bromo PEP dose-dependently reduced CFA-induced mechanical hypersensitivity. While being effective also at lower tested dosages of 1 and 3.3 mg/kg, 10 mg/kg of m-bromo PEP fully reversed CFA-induced mechanical hypersensitivity at 15 and 30 min after injection. The effect of m-bromo PEP after the dose of 10 mg/kg dissipated after 120 min after injection. In sham-treated mice 10 mg/kg m-bromo PEP did not alter von Frey responses, since m-bromo PEP at the tested dose and vehicle provided comparable responses. In addition, m-bromo PEP significantly reduced paw edema (, with mice treated with 10 mg/kg dose differing from the vehicle group. These results therefore corroborate previously published data demonstrating that p-CF_3 diEPP, a structurally similar α7 nAChR silent agonist, protects against inflammatory pain [30].

4. Discussion

The ability of the α7 nAChR to modulate inflammation is well established [56,57]. For instance, we and others have shown that the α7 nAChR protects against disease symptoms and pathology in EAE [2,4–6] and inflammatory pain [1] when it is activated by ligands such as nicotine or acetylcholine. The α7 nAChR could therefore serve as a molecular target for the treatment of many inflammatory and immune disorders. However, the pharmacological and cellular mechanisms by which these receptors modulate immune responses have not been clearly established to date. Immune cells are non-excitable, suggesting that nAChRs likely don’t exhibit the same well-characterized channel-dependent mechanisms of action that are observed in neurons. In addition, α7 nAChRs are quickly desensitized by acetylcholine and nicotine, and remain in this state for extended periods of time [24,25], especially at concentrations above 1 μM in the case of nicotine [16]. Many studies indeed show that nicotine exerts its anti-inflammatory effects at concentrations above 1 μM [2,3,11,55,58]. Assuming that α7 nAChRs assemble into functional pentamers as they do in neurons, this provides further evidence suggesting that the α7 nAChR channel must be closed or that the receptor must either be in a desensitized or other uncharacterized conformational state. The goal of this study was therefore to investigate this hypothesis.

Previously, we had shown that nicotine can modulate monocyte/macrophage numbers in a murine BMDM cell culture model via α7 and α9 nAChRs [55]. Although the general reduction in mean BMDM numbers did not reach statistical significance in the current study, this is likely due to the low sample numbers used in the preliminary experiments

presented in Fig. 1. Interestingly however, the pan-nAChR non-competitive antagonist reduced BMDM numbers. Ex vivo mecamylamine treatment, without the treatment of an agonist, also inhibited M1 BMDM numbers and cytokine production. Furthermore, treatment of EAE mice with mecamylamine ameliorated clinical scores, diminished the number of pro-inflammatory cells into the CNS and reduced the mRNA expression of multiple molecules necessary for immune cell recruitment, such as chemokines, integrins and metalloproteases. As a non-competitive antagonist, mecamylamine does not fully prevent binding of other ligands to the nAChR [60], since both molecules do not bind to the same site [61]. Moreover, non-competitive antagonists promote high agonist affinity states that are associated with receptor desensitization [62]. When mecamylamine and another nAChR ligand are both present, it is therefore possible that the nAChR favors the adoption of a desensitized, or similar closed-channel state that allows for nAChR-dependent anti-inflammatory effects.

Our data also show that mecamylamine alone exerts anti-inflammatory effects ex vivo and in vivo. These results could be explained by two scenarios: first, upon binding of mecamylamine to an allosteric site or within the channel pore, the receptor may adopt a conformational state similar to that of the desensitized receptor, possibly inducing downstream metabotropic signaling [62]. While mecamylamine is an antagonist from the canonical channel function perspective, it may instead act as an agonist in terms the metabotropic functions of the α7 nAChR. This may be especially true in immune cells, since the structure of nAChRs remains to be elucidated in these non-neuronal cells. Alternatively, there may be an alternate source of acetylcholine in bone marrow cell cultures or in vivo, which could bind to the nAChR concomitantly with mecamylamine. Although acetylcholine is abundantly produced in the CNS, its production has also been demonstrated in non-neuronal cells, such as T cells [63–67], natural killer cells [68] and endothelial cells [69]. Treatment of BMDMs or mice with mecamylamine in the presence of local acetylcholine production could therefore be sufficient to modulate inflammatory responses. Further studies will be necessary to investigate these possible mechanisms.

Previous studies found that mecamylamine reversed nicotine's and phosphocholine's effects on ATP-induced IL-1β production by the U937 macrophage cell line or mouse PBMCs, respectively [59,70]. The antagonist also prevented the protective effects of Rivastigmine, an acetylcholinesterase inhibitor, in EAE [71]. At first glance, our data contradict these previous findings, since we show that mecamylamine did not block nicotine's effects on pro-inflammatory BMDM numbers. In fact, we found that the drug instead acted similarly to nicotine by reducing pro-inflammatory BMDM numbers and by inhibiting TNFα secretion. These discrepancies could be explained by a few key differences between these previous studies and our own. First, we were unable to measure detectable levels of IL-1β in our LPS-induced BMDM model, while these other studies did not evaluate the effect of mecamylamine on TNFα secretion. Second, the previous studies used acute treatments of mecamylamine, whereas our experimental setup involved chronic mecamylamine treatment over the course of 54–72 h ex vivo or 16 days in vivo. It is therefore possible that mecamylamine affects BMDM numbers and phenotype ex vivo, pro-inflammatory cytokine production or EAE progression in vivo when chronically applied. Overall, further studies

will be necessary to consolidate the mechanisms of action of mecamylamine and its ability to modulate inflammation.

Another interesting observation from our mecamylamine treatment data is that the drug appears to exhibit a dose-dependent reduction in BMDM numbers, reaching a maximum effect at concentrations above 10 μM. While mecamylamine can non-competitively antagonize heteromeric nAChRs at lower concentrations, 10 μM or more are necessary for full antagonism of the α7 nAChR [14,72]. In combination with our data suggesting that receptor desensitization is responsible for downstream anti-inflammatory effects, this prompted us to investigate the ability of α7 nAChR-selective silent agonists to inhibit inflammation in the BMDM and EAE models.

We therefore made use of m-bromo PEP, a novel α7 nAChR-selective molecule [29] that induces very little α7 nAChR channel opening and prolonged receptor desensitization in Xenopus oocytes, as shown in Suppl. Fig. 1. Though m-bromo PEP does not act on α3β4 and α4β2 receptors, current tools do not allow us to assess its effects on α9-containing nAChRs. A first limitation of this study is that we are thus unable to exclude the possibility that m-bromo PEP may act via other nAChRs expressed by immune cells. Further studies are necessary to investigate the role of various nAChR subtypes in m-bromo PEP-mediated immune regulation. A second limitation is that we are unable to provide direct evidence that m-bromo PEP also acts as a silent agonist in monocytes and macrophages, since depolarization of macrophages in response to nAChR agonists cannot be measured. Since our findings demonstrate that mecamylamine and m-bromo PEP exhibit differences in their effects on immune cell function, it is likely that these two molecules modulate distinct intracellular signaling pathways, possibly via metabotropic receptor activity. This could be confirmed in future studies via the assessment of downstream signaling pathways that are modulated by m-bromo PEP in comparison to other types of nAChR ligands.

Nonetheless, our data show that this molecule was a very effective inhibitor of the inflammatory response, both ex vivo and in vivo. m-bromo PEP significantly reduced the numbers of BMDMs, especially the $CCR2^{+}Ly6C^{high}$ M1 cells. Interestingly however, the percentage of BMDMs that expressed high levels of CD80, a marker that is often associated with a pro-inflammatory phenotype [35,40,41], was increased by m-bromo PEP. On the other hand, the silent agonist also increased the $CD206^{high}$ BMDM population, a marker for the anti-inflammatory M2 phenotype [73]. m-bromo PEP also inhibited the expression of the LPS-induced pro-inflammatory cytokines TNFα and IL-6, while the anti-inflammatory cytokine IL-10 was also reduced after silent agonist treatment. These results suggest that m-bromo PEP has a direct effect on BMDM function, although its overall effect on the pro- vs anti-inflammatory balance is not clear ex vivo since the molecule inhibited the secretion of both pro- and anti-inflammatory cytokines.

In contrast, m-bromo PEP significantly ameliorated symptoms in EAE and CFA-induced inflammatory pain, two inflammatory mouse models. The drug also completely reversed the higher numbers of T and B cells that are present in the brain of EAE mice, both cell types that play a prominent role in MS pathology. The number of infiltrating monocytes was also significantly reduced by m-bromo PEP treatment. Even though the ratio of

M1:total infiltrating monocytes was not different in m-bromo PEP-treated EAE mice, we can conclude that the total number of M1 cells was nonetheless significantly lowered by the drug due to the reduction of total monocyte numbers. Finally, the lower proportions of microglia with respect to total leukocytes in EAE mice, an effect reversed by m-bromo PEP, can be attributed to the drug's inhibition of the large increase in proportions of other cell types making up the leukocyte population. Overall, our data thus suggest that the reduced clinical scores in EAE mice treated with m-bromo PEP are due to the inhibition or delay of pro-inflammatory cell recruitment into the CNS during the initial stages of the disease. Interestingly, m-bromo PEP inhibited the expression of the chemokines CCL2, CXCL2 and CCL19, all of which play important roles in the recruitment of inflammatory cells into the CNS. These findings are all in line with our previous study which used nicotine as a nAChR ligand [5]. On the other hand, the silent agonist did not affect CCL2-induced monocyte migration using an ex vivo assay. It should however be noted that the monocytes used were obtained from the bone marrow of naïve mice. Further studies are necessary to determine if m-bromo PEP can directly inhibit the migration of EAE-induced monocytes. Overall, these data suggest that in vivo, the effects of m-bromo PEP on pro-inflammatory cell recruitment to the CNS may be largely due to indirect mechanisms, such as the local expression of factors that promote cell recruitment within the CNS. It nonetheless remains likely that direct actions of the silent agonist on immune cells, such as observed with cytokine production ex vivo, play an important role in determining the drug's ability to protect against inflammatory disease pathology.

Overall, our data further strengthen the evidence that these effects are dependent on receptor desensitization, rather than channel opening [27,28,30,74]. Previous studies have also shown that nicotine and acetylcholine can modulate inflammatory signaling cascades, including the PI3K, Akt and MAPK pathways in lymphocytes [75], as well as NF-κB and the JAK2/STAT3 pathway in monocytes and macrophages [21,22,76]. Though traditionally viewed as nAChR agonists, nicotine and acetylcholine induce rapid desensitization of the α7 nAChR [24,25]. It is therefore likely that the silent agonist used in the present and past studies [27,29,30] also induce α7 nAChR-dependent metabotropic signaling mechanisms. However, further studies are necessary to investigate this hypothesis.

In summary, our data show that a silent agonist of α7 nAChRs inhibits inflammation, both in ex vivo models of BMDM function, and in vivo, using animal models of multiple sclerosis and inflammatory pain. Our results thus further support the hypothesis that nAChRs may modulate inflammation via receptor desensitization rather than canonical channel opening. α7 nAChR-selective silent agonists may thus be a novel source of anti-inflammatory compounds that could be used for the treatment of inflammatory disorders.

Supplementary Material

Refer to Web version on PubMed Central for supplementary material.

Acknowledgements

The authors would like to acknowledge Marc Surette, PhD (Université de Moncton) for kindly sharing his laboratory equipment, as well as Anick Beaulieu, M.Sc. (Université de Moncton) and Crystal Morrison, CVT (Université de Moncton) for technical expertise.

Funding

This work was supported by grants from the MS Society of Canada (EGID2995) and NIH grant RO1 GM57481.

References

(1). Gao B, Hierl M, Clarkin K, Juan T, Nguyen H, van der Valk M, et al. , 2010 4. Pharmacological effects of nonselective and subtype-selective nicotinic acetylcholine receptor agonists in animal models of persistent pain. Pain 149 (1), 33–49. [PubMed: 20167427]

(2). Hao J, Simard AR, Turner GH, Wu J, Whiteaker P, Lukas RJ, et al. , 2011 1. Attenuation of CNS inflammatory responses by nicotine involves α7 and non-α7 nicotinic receptors. Exp. Neurol 227 (1), 110–119. [PubMed: 20932827]

(3). Shi F-D, Piao W-H, Kuo Y-P, Campagnolo DI, Vollmer TL, Lukas RJ, 2009. Nicotinic attenuation of central nervous system inflammation and autoimmunity. J. Immunol 182 (3), 1730–1739. [PubMed: 19155522]

(4). Simard AR, Gan Y, St-Pierre S, Kousari A, Patel V, Whiteaker P, et al. , 2013 3. Differential modulation of EAE by α9*- and β2*-nicotinic acetylcholine receptors. Immunol. Cell Biol 91 (3), 195–200. [PubMed: 23399696]

(5). Jiang W, St-Pierre S, Roy P, Morley BJ, Hao J, Simard AR, 2016 3 1. Infiltration of CCR2 $^{+}$ Ly6C ^{high} Proinflammatory Monocytes and Neutrophils into the Central Nervous System Is Modulated by Nicotinic Acetylcholine Receptors in a Model of Multiple Sclerosis. J. Immunol 196 (5), 2095–2108. [PubMed: 26810225]

(6). Nizri E, Irony-Tur-Sinai M, Lory O, Orr-Urtreger A, Lavi E, Brenner T, 2009 11 15. Activation of the Cholinergic Anti-Inflammatory System by Nicotine Attenuates Neuroinflammation via Suppression of Th1 and Th17 Responses. J. Immunol 183 (10), 6681–6688. [PubMed: 19846875]

(7). Bruchfeld A, Goldstein RS, Chavan S, Patel NB, Rosas-Ballina M, Kohn N, et al. , 2010 7. Whole blood cytokine attenuation by cholinergic agonists ex vivo and relationship to vagus nerve activity in rheumatoid arthritis. J. Intern. Med 268 (1), 94–101. [PubMed: 20337855]

(8). De Rosa MJ, Esandi M. del C., Garelli A, Rayes D, Bouzat C, 2005 3. Relationship between α7 nAChR and apoptosis in human lymphocytes. J. Neuroimmunol 160 (1–2), 154–161. [PubMed: 15710468]

(9). Yoshikawa H, Kurokawa M, Ozaki N, Nara K, Atou K, Takada E, et al. , 2006 10. Nicotine inhibits the production of proinflammatory mediators in human monocytes by suppression of I-κB phosphorylation and nuclear factor-κB transcriptional activity through nicotinic acetylcholine receptor α7. Clin. Exp. Immunol 146 (1), 116–123. [PubMed: 16968406]

(10). Patton GW, Powell DA, Hakki A, Friedman H, Pross S, 2006 1. Nicotine modulation of cytokine induction by LPS-stimulated human monocytes and coronary artery endothelial cells. Int. Immunopharmacol 6 (1), 26–35. [PubMed: 16332510]

(11). Takahashi HK, Iwagaki H, Hamano R, Kanke T, Liu K, Sadamori H, et al. , 2007 3. The immunosuppressive effects of nicotine during human mixed lymphocyte reaction. Eur. J. Pharmacol 559 (1), 69–74. [PubMed: 17254563]

(12). Hedström AK, Bäärnhielm M, Olsson T, Alfredsson L, 2009 9 1. Tobacco smoking, but not Swedish snuff use, increases the risk of multiple sclerosis. Neurology 73 (9), 696–701. [PubMed: 19720976]

(13). Hedström A, Hillert J, Olsson T, Alfredsson L, 2013 7. Nicotine might have a protective effect in the etiology of multiple sclerosis. Mult. Scler. J 19 (8), 1009–1013.

(14). Jensen AA, Frølund B, Liljefors T, Krogsgaard-Larsen P, 2005 7. Neuronal Nicotinic Acetylcholine Receptors: Structural Revelations, Target Identifications, and Therapeutic Inspirations. J. Med. Chem 48 (15), 4705–4745. [PubMed: 16033252]

(15). Papke RL, Meyer E, Nutter T, Uteshev VV, 2000 3 30. α7 Receptor-selective agonists and modes of α7 receptor activation. Eur. J. Pharmacol 393 (1), 179–195. [PubMed: 10771012]

(16). Papke RL, Kem WR, Soti F, Lopez-Hernandez GY, Horenstein NA, 2009 5 1. Activation and Desensitization of Nicotinic α7-type Acetylcholine Receptors by Benzylidene Anabaseines and Nicotine. J. Pharmacol. Exp. Ther 329 (2), 791–807. [PubMed: 19223664]

(17). Wang H, Yu M, Ochani M, Amella CA, et al. , 2003. Nicotinic acetylcholine receptor alpha7 subunit is an essential regulator of inflammation. Nat. Lond 421 (6921), 384–388. [PubMed: 12508119]

(18). De Rosa MJ, Dionisio L, Agriello E, Bouzat C, Esandi MC, 2009 9. Alpha 7 nicotinic acetylcholine receptor modulates lymphocyte activation. Life Sci 85 (11–12), 444–449. [PubMed: 19632243]

(19). Corradi J, Bouzat C, 2016 9 1. Understanding the Bases of Function and Modulation of α7 Nicotinic Receptors: Implications for Drug Discovery. Mol. Pharmacol 90 (3), 288–299. [PubMed: 27190210]

(20). Galitovskiy V, Qian J, Chernyavsky AI, Marchenko S, Gindi V, Edwards RA,et al. , 2011 9 1. Cytokine-Induced Alterations of α7 Nicotinic Receptor in Colonic CD4 T Cells Mediate Dichotomous Response to Nicotine in Murine Models of Th1/Th17- versus Th2-Mediated Colitis. J. Immunol 187 (5), 2677–2687. [PubMed: 21784975]

(21). de Jonge WJ, van der Zanden EP, The FO, Bijlsma MF, van Westerloo DJ, Bennink RJ, et al. , 2005 8. Stimulation of the vagus nerve attenuates macrophage activation by activating the Jak2-STAT3 signaling pathway. Nat. Immunol 6(8), 844–851. [PubMed: 16025117]

(22). Wang H, Liao H, Ochani M, Justiniani M, Lin X, Yang L, et al. , 2004. Cholinergic agonists inhibit HMGB1 release and improve survival in experimental sepsis. Nat. Med 10 (11), 1216. [PubMed: 15502843]

(23). Zanetti SR, Ziblat A, Torres NI, Zwirner NW, Bouzat C, 2016 8 5. Expression and Functional Role of α7 Nicotinic Receptor in Human Cytokine-stimulated Natural Killer (NK) Cells. J. Biol. Chem 291 (32), 16541–16552. [PubMed: 27284006]

(24). Papke RL, 2014 5. Merging old and new perspectives on nicotinic acetylcholine receptors. Biochem. Pharmacol 89 (1), 1–11. [PubMed: 24486571]

(25). Horenstein NA, Papke RL, 2017. Anti-inflammatory Silent Agonists. ACS Med. Chem. Lett. [Internet] 2017 9 26; Available from: 10.1021/acsmedchemlett.7b00368.

(26). Chojnacka K, Papke RL, Horenstein NA, 2013 7 15. Synthesis and evaluation of a conditionally-silent agonist for the α7 nicotinic acetylcholine receptor. Bioorg. Med. Chem. Lett 23 (14), 4145–4149. [PubMed: 23746476]

(27). Papke RL, Bagdas D, Kulkarni AR, Gould T, AlSharari SD, Thakur GA, et al. , 2015 4. The analgesic-like properties of the alpha7 nAChR silent agonist NS6740 is associated with non-conducting conformations of the receptor. Neuropharmacology 91, 34–42. [PubMed: 25497451]

(28). van Maanen MA, Papke RL, Koopman FA, Koepke J, Bevaart L, Clark R, et al. , 2015. Two Novel α7 Nicotinic Acetylcholine Receptor Ligands. In Vitro Properties and Their Efficacy in Collagen-Induced Arthritis in Mice. Heymann D, editor. PLOS ONE 10 (1), e0116227. [PubMed: 25617631]

(29). Quadri M, Papke RL, Horenstein NA, 2016 1 15. Dissection of N, N-diethyl-N′-phenylpiperazines as α7 nicotinic receptor silent agonists. Bioorg. Med. Chem 24 (2), 286–293. [PubMed: 26707847]

(30). Quadri M, Bagdas D, Toma W, Stokes C, Horenstein NA, Damaj MI, et al. , 2018. The antinociceptive and anti-inflammatory properties of the α7 nAChR weak partial agonist p-CF3 N,N-diethyl-N'-phenylpiperazine. J. Pharmacol. Exp. Ther 2018 1 1;jpet.118.249904.

(31). Mishra MK, Yong VW, 2016 8 12. Myeloid cells - targets of medication in multiple sclerosis. Nat Rev Neurol. 12 (9), 539–551. [PubMed: 27514287]

(32). Herz J, Filiano AJ, Smith A, Yogev N, Kipnis J, 2017 6 20. Myeloid Cells in the Central Nervous System. Immunity 46 (6), 943–956. [PubMed: 28636961]

(33). Brück W, Sommermeier N, Bergmann M, Zettl U, Goebel HH, Kretzschmar HA, et al. , 1996 10 1. CHAPTER 14 - Macrophages in Multiple Sclerosis. Immunobiology 195 (4), 588–600. [PubMed: 8933159]

(34). Henderson APD, Barnett MH, Parratt JDE, Prineas JW, 2009. Multiple sclerosis: distribution of inflammatory cells in newly forming lesions. Ann. Neurol 66 (6), 739–753. [PubMed: 20035511]

(35). Auffray C, Sieweke MH, Geissmann F, 2009 4. Blood Monocytes: Development, Heterogeneity, and Relationship with Dendritic Cells. Annu. Rev. Immunol 27 (1), 669–692. [PubMed: 19132917]

(36). Martinez FO, Gordon S, 2017. The M1 and M2 paradigm of macrophage activation: time for reassessment. F1000prime Rep [Internet]. 2014 [cited 2017 Jun 26];6. Available from: https://www.ncbi.nlm.nih.gov/pmc/articles/PMC3944738/.

(37). Mikita J, Dubourdieu-Cassagno N, Deloire MS, Vekris A, Biran M, Raffard G,et al. , 2011 1. Altered M1/M2 activation patterns of monocytes in severe relapsing experimental rat model of multiple sclerosis. Amelioration of clinical status by M2 activated monocyte administration. Mult Scler J. 17 (1), 2–15.

(38). Weber MS, Prod'homme T, Youssef S, Dunn SE, Rundle CD, Lee L, et al. , 2007 9. Type II monocytes modulate T cell-mediated central nervous system autoimmune disease. Nat. Med 13 (8), 935–943. [PubMed: 17676050]

(39). Murray P, Allen J, Biswas S, Fisher E, Gilroy D, Goerdt S, et al. , 2014 7. Macrophage Activation and Polarization: Nomenclature and Experimental Guidelines. Immunity 41 (1), 14–20. [PubMed: 25035950]

(40). Geissmann F, Jung S, Littman DR, 2003. Blood monocytes consist of two principal subsets with distinct migratory properties. Immunity 19 (1), 71–82. [PubMed: 12871640]

(41). Sunderkötter C, Nikolic T, Dillon MJ, Van Rooijen N, Stehling M, Drevets DA, et al. , 2004. Subpopulations of mouse blood monocytes differ in maturation stage and inflammatory response. J. Immunol 172 (7), 4410–4417. [PubMed: 15034056]

(42). Serbina NV, Pamer EG, 2006 3. Monocyte emigration from bone marrow during bacterial infection requires signals mediated by chemokine receptor CCR2. Nat. Immunol 7 (3), 311. [PubMed: 16462739]

(43). Clarkson BD, Walker A, Harris MG, Rayasam A, Sandor M, Fabry Z, 1950. 2015,. CCR2-dependent dendritic cell accumulation in CNS during early effector EAE is essential for effector T cell restimulation in situ and disease progression. J. Immunol. Baltim. Md 194 (2), 531–541.

(44). Mildner A, Mack M, Schmidt H, Brück W, Djukic M, Zabel MD, et al. , 2009 9 1. CCR2+Ly-6Chi monocytes are crucial for the effector phase of autoimmunity in the central nervous system. Brain 132 (9), 2487–2500. [PubMed: 19531531]

(45). Hurst RS, Hajós M, Raggenbass M, Wall TM, Higdon NR, Lawson JA, et al. , 2005 4 27. A novel positive allosteric modulator of the alpha7 neuronal nicotinic acetylcholine receptor: in vitro and in vivo characterization. J. Neurosci. Off. J. Soc. Neurosci 25 (17), 4396–4405.

(46). Halevi S, Yassin L, Eshel M, Sala F, Sala S, Criado M, et al. , 2003. Conservation within the RIC-3 gene family. Effectors of mammalian nicotinic acetylcholine receptor expression. J. Biol. Chem 278 (36), 34411–34417. [PubMed: 12821669]

(47). Papke RL, Stokes C, 2010 5. Working with OpusXpress: methods for high volume oocyte experiments. Methods San Diego Calif. 51 (1), 121–133.

(48). Papke RL, Porter Papke JK, 2002 9. Comparative pharmacology of rat and human alpha7 nAChR conducted with net charge analysis. Br. J. Pharmacol 137 (1), 49–61. [PubMed: 12183330]

(49). Gao Z, Nissen JC, Ji K, Tsirka SE, 2014 9. The Experimental Autoimmune Encephalomyelitis Disease Course Is Modulated by Nicotine and Other Cigarette Smoke Components. Mengod G, editor. PLoS ONE 9 (9), e107979. [PubMed: 25250777]

(50). Matsuda R, Kezuka T, Nishiyama C, Usui Y, Matsunaga Y, Okunuki Y, et al. , 2012 8 1. Suppression of Murine Experimental Autoimmune Optic Neuritis by Mature Dendritic Cells Transfected with Calcitonin Gene-Related Peptide Gene. Invest. Ophthalmol. Vis. Sci 53 (9), 5475–5485. [PubMed: 22807299]

(51). Hartung JE, Eskew O, Wong T, Tchivileva IE, Oladosu FA, O'Buckley SC, et al. , 2015 11. Nuclear factor-kappa B regulates pain and COMT expression in a rodent model of inflammation. Brain Behav. Immun 50, 196–202. [PubMed: 26187567]

(52). Chaplan SR, Bach FW, Pogrel JW, Chung JM, Yaksh TL, 1994 7. Quantitative assessment of tactile allodynia in the rat paw. J. Neurosci. Methods 53 (1), 55–63. [PubMed: 7990513]

(53). Bagdas D, AlSharari SD, Freitas K, Tracy M, Damaj MI, 2015 10 15. The role of alpha5 nicotinic acetylcholine receptors in mouse models of chronic inflammatory and neuropathic pain. Biochem. Pharmacol 97 (4), 590–600. [PubMed: 25931144]

(54). Dixon WJ, 1965 12 1. The Up-and-Down Method for Small Samples. J. Am. Stat. Assoc60 (312), 967–978.

(55). St-Pierre S, Jiang W, Roy P, Champigny C, LeBlanc É, Morley BJ, et al. , 2016. Nicotinic Acetylcholine Receptors Modulate Bone Marrow-Derived Pro-Inflammatory Monocyte Production and Survival. Chellappan SP, editor. PLOS ONE 11 (2), e0150230. [PubMed: 26925951]

(56). Bagdas D, Gurun MS, Flood P, Papke RL, Damaj MI, 2018 5. New Insights on Neuronal Nicotinic Acetylcholine Receptors as Targets for Pain and Inflammation: A Focus on α7 nAChRs. Curr. Neuropharmacol 16 (4), 415–425. [PubMed: 28820052]

(57). Liu Q, Whiteaker P, Morley BJ, Shi F-D, Lukas RJ, 2017. Distinctive Roles for α7*-and α9*-Nicotinic Acetylcholine Receptors in Inflammatory and Autoimmune Responses in the Murine Experimental Autoimmune Encephalomyelitis Model of Multiple Sclerosis. Front. Cell. Neurosci. [Internet] 2017 [cited 2019 Aug 2];11. Available from: https://www.frontiersin.org/articles/10.3389/fncel.2017.00287/full.

(58). Takahashi HK, Iwagaki H, Hamano R, Yoshino T, Tanaka N, Nishibori M, 2006 8 18. Effect of nicotine on IL-18-initiated immune response in human monocytes. J. Leukoc. Biol 80 (6), 1388–1394. [PubMed: 16966384]

(59). Hecker A, Küllmar M, Wilker S, Richter K, Zakrzewicz A, Atanasova S, et al. , 2015 9 1. Phosphocholine-Modified Macromolecules and Canonical Nicotinic Agonists Inhibit ATP-Induced IL-1β Release. J. Immunol 195 (5), 2325–2334. [PubMed: 26202987]

(60). Loiacono R, Stephenson J, Stevenson J, Mitchelson F, 1993 9. Multiple binding sites for nicotine receptor antagonists in inhibiting [3H](−)-nicotine binding in rat cortex. Neuropharmacology 32 (9), 847–853. [PubMed: 8232788]

(61). Webster JC, Francis MM, Porter JK, Robinson G, Stokes C, Horenstein B, et al. , 1999. Antagonist activities of mecamylamine and nicotine show reciprocal dependence on beta subunit sequence in the second transmembrane domain. Br. J. Pharmacol 127 (6), 1337–1348. [PubMed: 10455283]

(62). Bertrand D, Ballivet M, Rungger D, 1990 3 1. Activation and blocking of neuronal nicotinic acetylcholine receptor reconstituted in Xenopus oocytes. Proc. Natl. Acad. Sci 87 (5), 1993–1997. [PubMed: 1968642]

(63). Kawashima K, Fujii T, 2004. Expression of non-neuronal acetylcholine in lymphocytes and its contribution to the regulation of immune function. Front Biosci J Virtual Libr 9, 2063–2085.

(64). Kawashima K, Fujii T, 2000. Extraneuronal cholinergic system in lymphocytes. Pharmacol. Ther 86 (1), 29–48. [PubMed: 10760545]

(65). Fujii T, Mashimo M, Moriwaki Y, Misawa H, Ono S, Horiguchi K, et al. , 2017. Expression and Function of the Cholinergic System in Immune Cells. Front. Immunol 8, 1085. [PubMed: 28932225]

(66). Rosas-Ballina M, Olofsson PS, Ochani M, Valdes-Ferrer SI, Levine YA, Reardon C, et al. , 2011 10 7. Acetylcholine-Synthesizing T Cells Relay Neural Signals in a Vagus Nerve Circuit. Science 334 (6052), 98–101. [PubMed: 21921156]

(67). Reardon C, Duncan GS, Brüstle A, Brenner D, Tusche MW, Olofsson PS, et al. , 2013 1 22. Lymphocyte-derived ACh regulates local innate but not adaptive immunity. Proc. Natl. Acad. Sci 110 (4), 1410–1415. [PubMed: 23297238]

(68). Jiang W, Li D, Han R, Zhang C, Jin W-N, Wood K, et al. , 2017 7 25. Acetylcholine-producing NK cells attenuate CNS inflammation via modulation of infiltrating monocytes/macrophages. Proc. Natl. Acad. Sci 114 (30), E6202–E6211. [PubMed: 28696300]

(69). Wilson C, Lee MD, McCarron JG, 2016 12 15. Acetylcholine released by endothelial cells facilitates flow-mediated dilatation. J. Physiol 594 (24), 7267–7307. [PubMed: 27730645]

(70). Richter K, Mathes V, Fronius M, Althaus M, Hecker A, Krasteva-Christ G, et al. , 2016. Phosphocholine – an agonist of metabotropic but not of ionotropic functions of α9-containing nicotinic acetylcholine receptors. Available from. Sci Rep [Internet]. 6. http://www.ncbi.nlm.nih.gov/pmc/articles/PMC4923896/.

(71). Nizri E, Irony-Tur-Sinai M, Faranesh N, Lavon I, Lavi E, Weinstock M, et al. , 2008 10. Suppression of neuroinflammation and immunomodulation by the acetylcholinesterase inhibitor rivastigmine. J. Neuroimmunol 203 (1), 12–22. [PubMed: 18692909]

(72). Chavez-Noriega LE, Crona JH, Washburn MS, Urrutia A, Elliott KJ, Johnson EC, 1997 1. Pharmacological characterization of recombinant human neuronal nicotinic acetylcholine receptors h alpha 2 beta 2, h alpha 2 beta 4, h alpha 3 beta 2, h alpha 3 beta 4, h alpha 4 beta 2, h alpha 4 beta 4 and h alpha 7 expressed in Xenopus oocytes. J. Pharmacol. Exp. Ther 280 (1), 346–356. [PubMed: 8996215]

(73). Stein M, Keshav S, Harris N, Gordon S, 1992. Interleukin 4 potently enhances murine macrophage mannose receptor activity: a marker of alternative immunologic macrophage activation. J. Exp. Med 176 (1), 287–292. [PubMed: 1613462]

(74). Thomsen MS, Mikkelsen JD, 2012 10. The α7 nicotinic acetylcholine receptor ligands methyllycaconitine, NS6740 and GTS-21 reduce lipopolysaccharide-induced TNF-α release from microglia. J. Neuroimmunol 251 (1–2), 65–72. [PubMed: 22884467]

(75). Aicher A, Heeschen C, Mohaupt M, Cooke JP, Zeiher AM, Dimmeler S, 2003 2 4. Nicotine Strongly Activates Dendritic Cell-Mediated Adaptive Immunity: Potential Role for Progression of Atherosclerotic Lesions. Circulation 107 (4), 604–611. [PubMed: 12566374]

(76). Saeed RW, Varma S, Peng-Nemeroff T, Sherry B, Balakhaneh D, Huston J, et al. , 2005 4 4. Cholinergic stimulation blocks endothelial cell activation and leukocyte recruitment during inflammation. J. Exp. Med 201 (7), 1113–1123. [PubMed: 15809354]

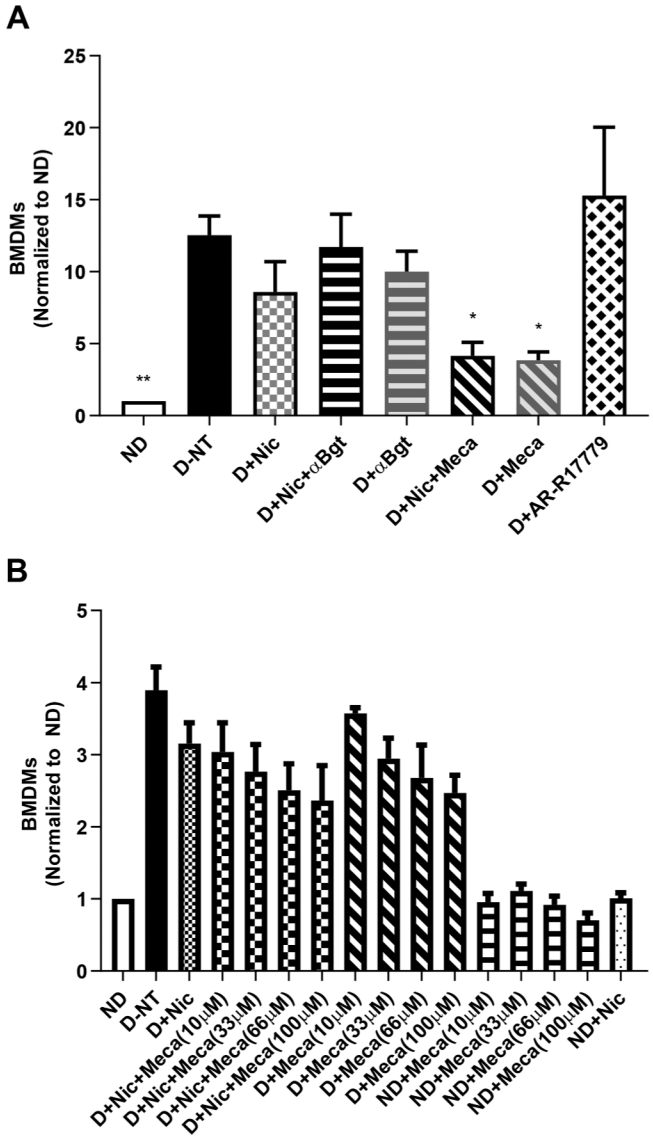

Fig. 1.

Mecamylamine reduces BMDM numbers. Bone marrow cells were freshly isolated from C57BL/6J mice. Cells from each individual mouse were separated and cultured for 3 days in the following conditions: non-differentiated (ND), with M-CSF and IFNγ to induce M1 BMDM differentiation (D), without drug treatment (NT), with nicotine (Nic), αBungarotoxin (αBgt), mecamylamine (Meca) or AR-R17779. Cells were then analyzed by flow cytometry to identify and quantify BMDMs. A, The effects of nicotine, αBgt, mecamylamine and AR-R17779 on BMDM numbers (n = 4). B, Dose-response effects of mecamylamine on BMDM numbers (n = 3). Data presented are means ± SEM. *P < 0.05; **P < 0.01 vs D-NT (Kruskal-Wallis one-way ANOVA, multiple comparisons with Dunn's correction).

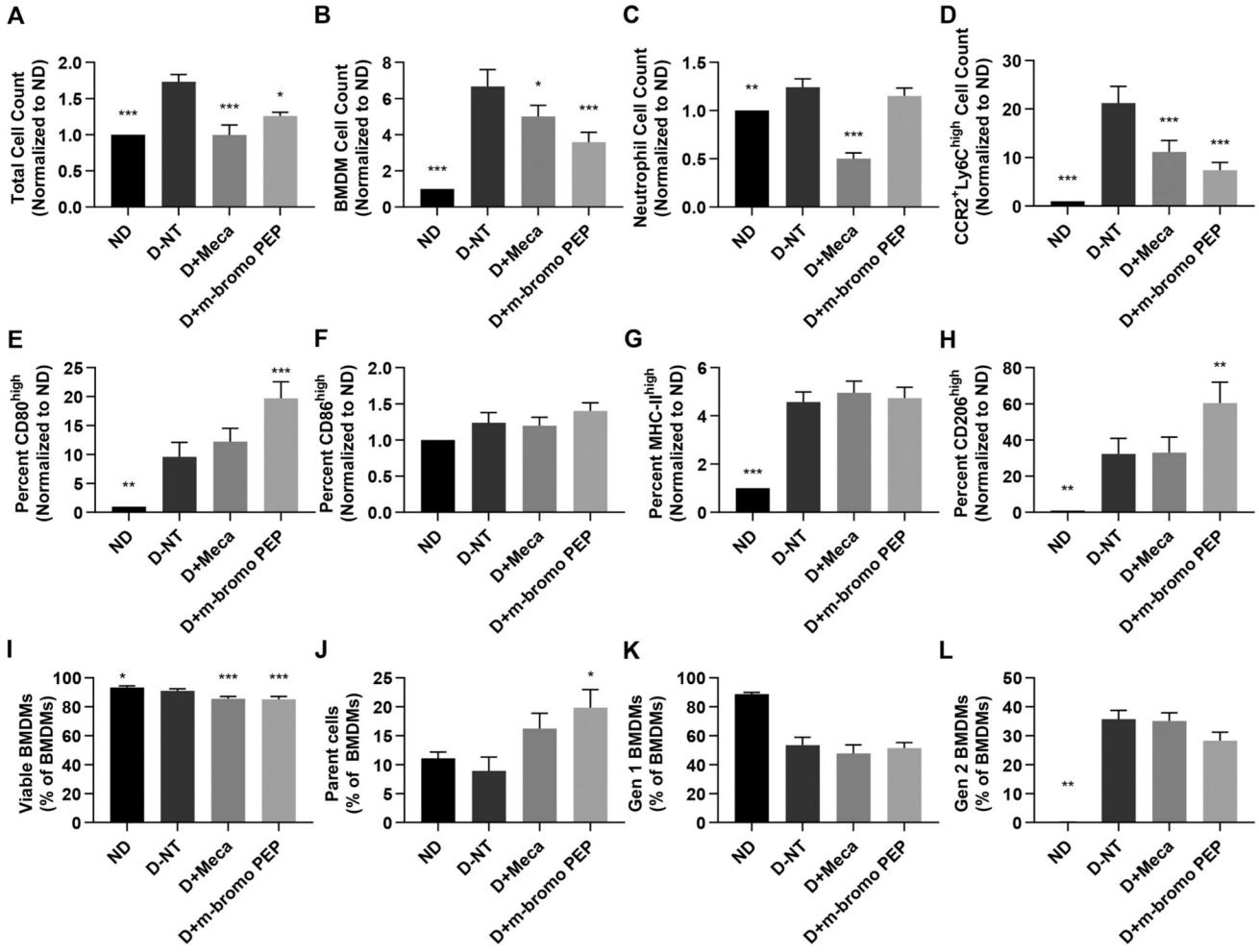

Fig. 2.

Mecamylamine and m-bromo PEP alter the abundance and phenotype of mouse BMDMs. Bone marrow cells were freshly isolated from C57BL/6J mice. Cells from each individual mouse were separated and cultured for 3 days in one of the following four conditions: non-differentiated (ND), in the presence of M-CSF and IFNγ to induce M1 BMDM differentiation with no drug treatment (D-NT), M1 differentiation with 100 μM mecamylamine (D + Meca) or M1 differentiation with 100 μM m-bromo PEP (D + m-bromo PEP). Cells were counted manually and further analyzed by flow cytometry. Data from panels A-H were normalized to the ND control. A, Total cell counts following the 3 days of cell culture (n = 8). B-D, Total BMDM (B, n = 9), neutrophil (C, n = 8) and M1 ($CCR2^{+}Ly\text{-}6C^{high}$) BMDM (D, n = 9) cell numbers in each treatment group. E-H, Proportions of BMDMs that express high levels of CD80 (E, n = 8), CD86 (F, n = 8), MHC-II (G, n = 9) and CD206 (H, n = 9). I, Proportions of viable BMDMs (n = 8). J-L, Proportions of BMDMs that were parent cells (J, n = 4), 1st generation cells (K, n = 4) or 2nd generation cells (L, n = 4) after the 3 days of culture. Data are presented as means ± SEM. For A-I, data were analyzed by repeated-measures one-way ANOVA with multiple comparisons using Dunnett's correction. For J-L, data were analyzed using the Friedman test

with Dunn's correction for multiple comparisons. *P < 0.05; **P < 0.01; ***P < 0.001 vs D-NT.

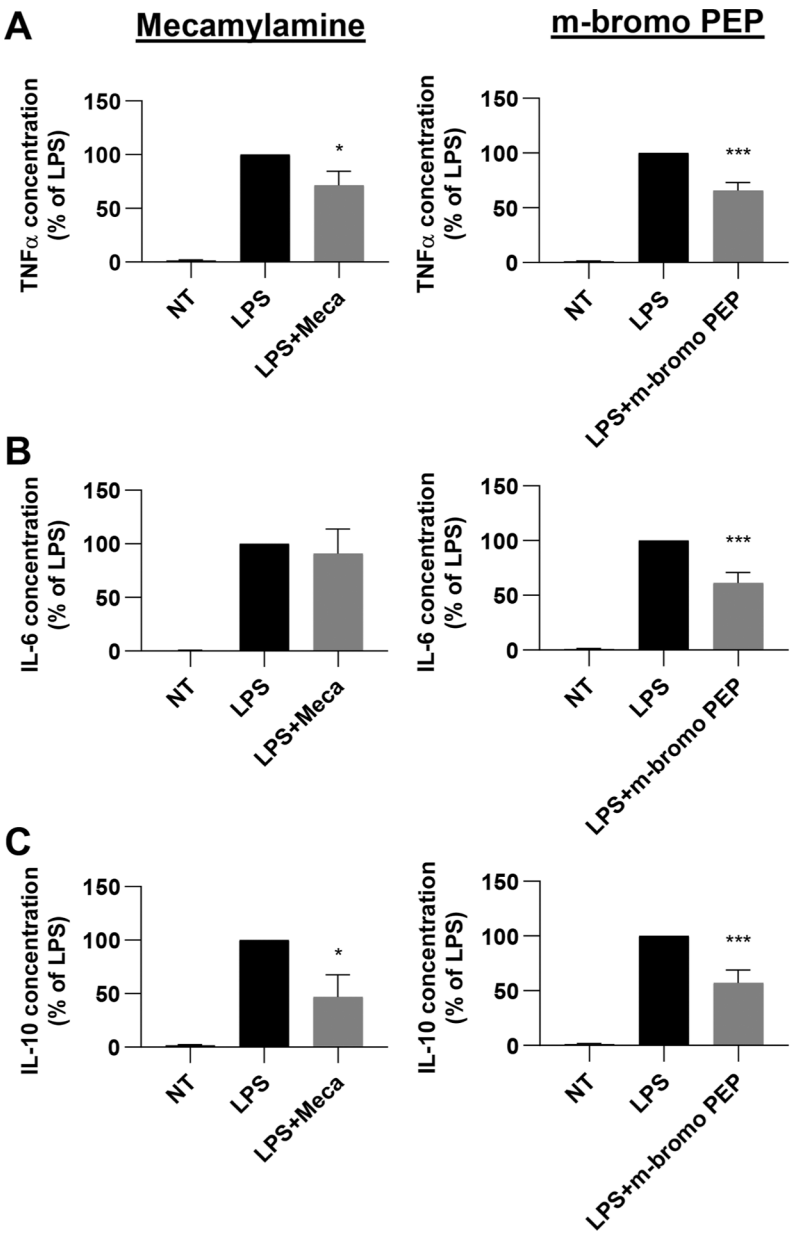

Fig. 3.

LPS-induced cytokine expression by BMDMs is modulated by m-bromo PEP and mecamylamine. Bone marrow cells were cultured for 48 h in the presence of M−CSF and IFNγ and then stimulated with LPS for 6 h. Cells were treated with or without mecamylamine (n = 9) or m-bromo PEP (n = 14) throughout the experiment. A-C, TNFα (A), IL-6 (B) and IL-10 (C) were then assessed in the supernatant. Cytokine concentrations were normalized to the LPS group (cells differentiated with M-CSF + IFNγ and stimulated with LPS). Data are presented as means ± SEM. *P < 0.05; **P < 0.01; ***P < 0.001 vs LPS control group (Repeated-measures one-way ANOVA, multiple comparisons with Dunnett's correction).

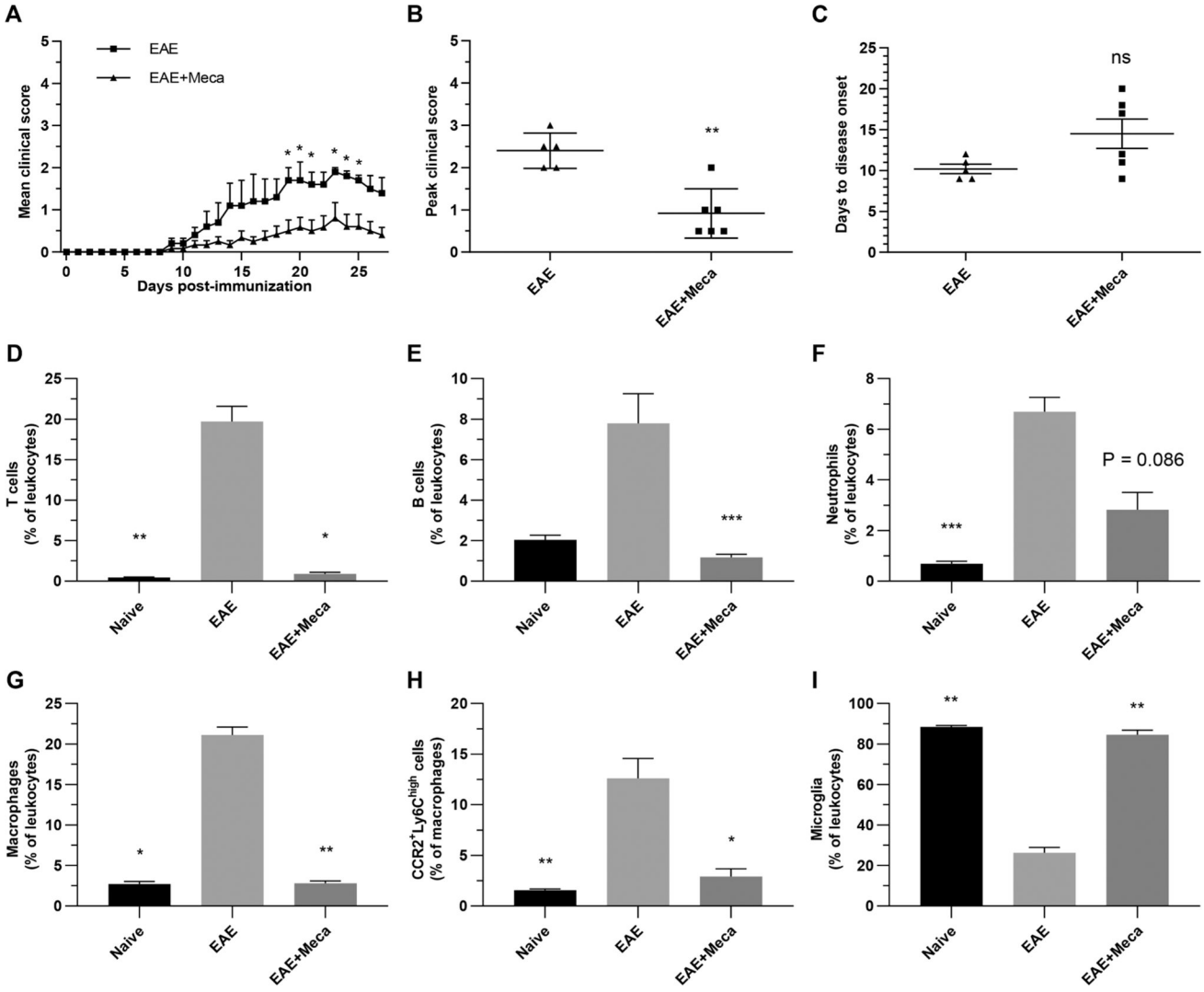

Fig. 4.

Mecamylamine reduces EAE clinical scores and immune cell infiltration into the CNS. A-C, Mice were immunized with $MOG_{35–55}$ (EAE; n = 5) and treated with 6.5 mg/kg/day mecamylamine (EAE + Meca; n = 6) via osmotic pumps from day -1 to day 16. Disease severity was scored each day for 28 days (A), while mean peak clinical scores (B) and days to disease onset (C) were calculated for both groups. Data are presented as means ± SEM. *P < 0.05; **P < 0.01 (In A, Mann-Whitney *U* test for global effect, followed by Multiple t tests with Holm-Sidak's correction; In B and C, Mann-Whitney *U* test, two tailed). D-I, In a separate experiment EAE (n = 8) and EAE + Meca (n = 6) mice were euthanized on day 13. Naive mice were used as controls (n = 4). Myelin debris were removed, and the proportions of various immune cells, with respect to total leukocytes, were determined in each brain by flow cytometry. Leukocytes were identified as T cells (D), B cells (E), neutrophils (F), infiltrating monocytes (G) and microglia (I). The proportions of infiltrating monocytes that were $CCR2^{+}Ly6C^{high}$ cells were also assessed (H). Data presented are means ± SEM. *P < 0.05; **P < 0.01; ***P < 0.001 vs EAE (Kruskal-Wallis one-way ANOVA, multiple comparisons with Dunn's correction).

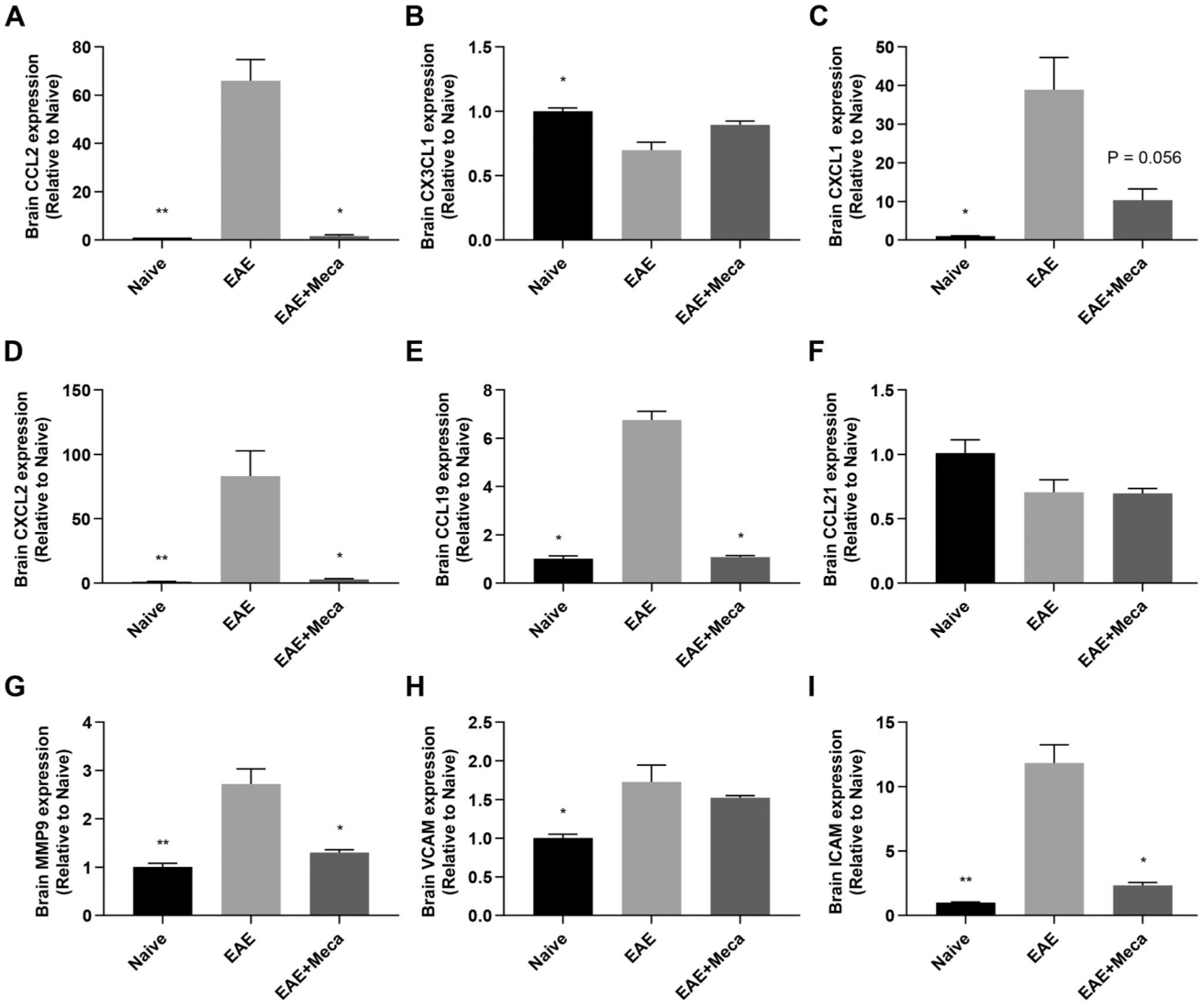

Fig. 5.

mRNA expression of genes important for immune cell infiltration into the CNS are inhibited by mecamylamine. Total RNA was purified from the brains of naive (n = 4), EAE (n = 8) and EAE + Meca (n = 6) mice at day 13 post immunization, and mRNA expression of several immune cell recruitment genes were assessed by qRT-PCR. A-F, relative mRNA expression for the chemokines CCL2 (A), CX3CL1 (B), CXCL1 (C), CXCL2 (D), CCL19 (E) and CCL21 (F) are shown. G-I, The matrix metalloproteinase MMP-9 (G), and the adhesion molecules VCAM (H) and ICAM (I) are also depicted. Data are presented as mean ± SEM. *P < 0.05; **P < 0.01; ***P < 0.001 vs EAE (Kruskal-Wallis one-way ANOVA, multiple comparisons with Dunn's correction).

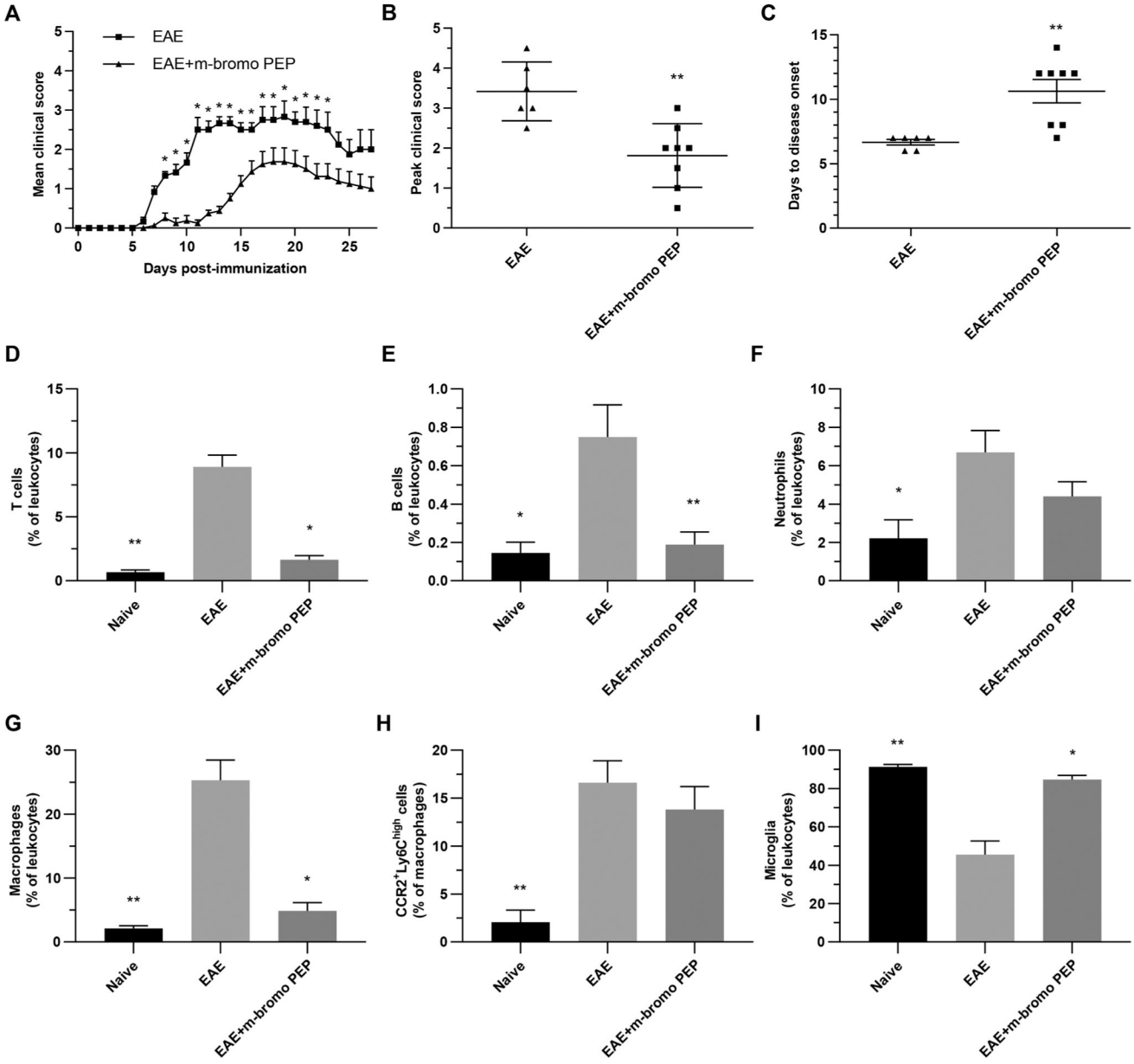

Fig. 6.

m-bromo PEP reduces EAE clinical scores and immune cell infiltration into the CNS. A-C, Mice were immunized with $MOG_{35–55}$ (EAE; n = 6) and treated with 6 mg/kg/day m-bromo PEP (EAE + m-bromo PEP; n = 8) via osmotic pumps from day -1 to day 16. Disease severity was scored each day for 28 days (A), while mean peak clinical scores (B) and days to disease onset (C) were calculated for both groups. Data are presented as mean ± SEM. *P < 0.05; **P < 0.01 (In A, Mann-Whitney *U* test for global effect, followed by Multiple t tests with Holm-Sidak's correction; In B and C, Mann-Whitney *U* test, two tailed). D-I, In a separate experiment EAE (n = 7) and EAE + m-bromo PEP (n = 7) mice were euthanized on day 16. Naive mice were used as controls (n = 4). Myelin debris were removed, and the proportions of various immune cells, with respect to total leukocytes, were determined in each brain by flow cytometry. Leukocytes were identified as T cells (D), B cells (E),

neutrophils (F), infiltrating monocytes (G) and microglia (I). The proportions of infiltrating monocytes that were $CCR2^{+}Ly6C^{high}$ cells were also assessed (H). Data presented are means ± SEM. *P < 0.05; **P < 0.01 vs EAE (Kruskal-Wallis one-way ANOVA, multiple comparisons with Dunn's correction).

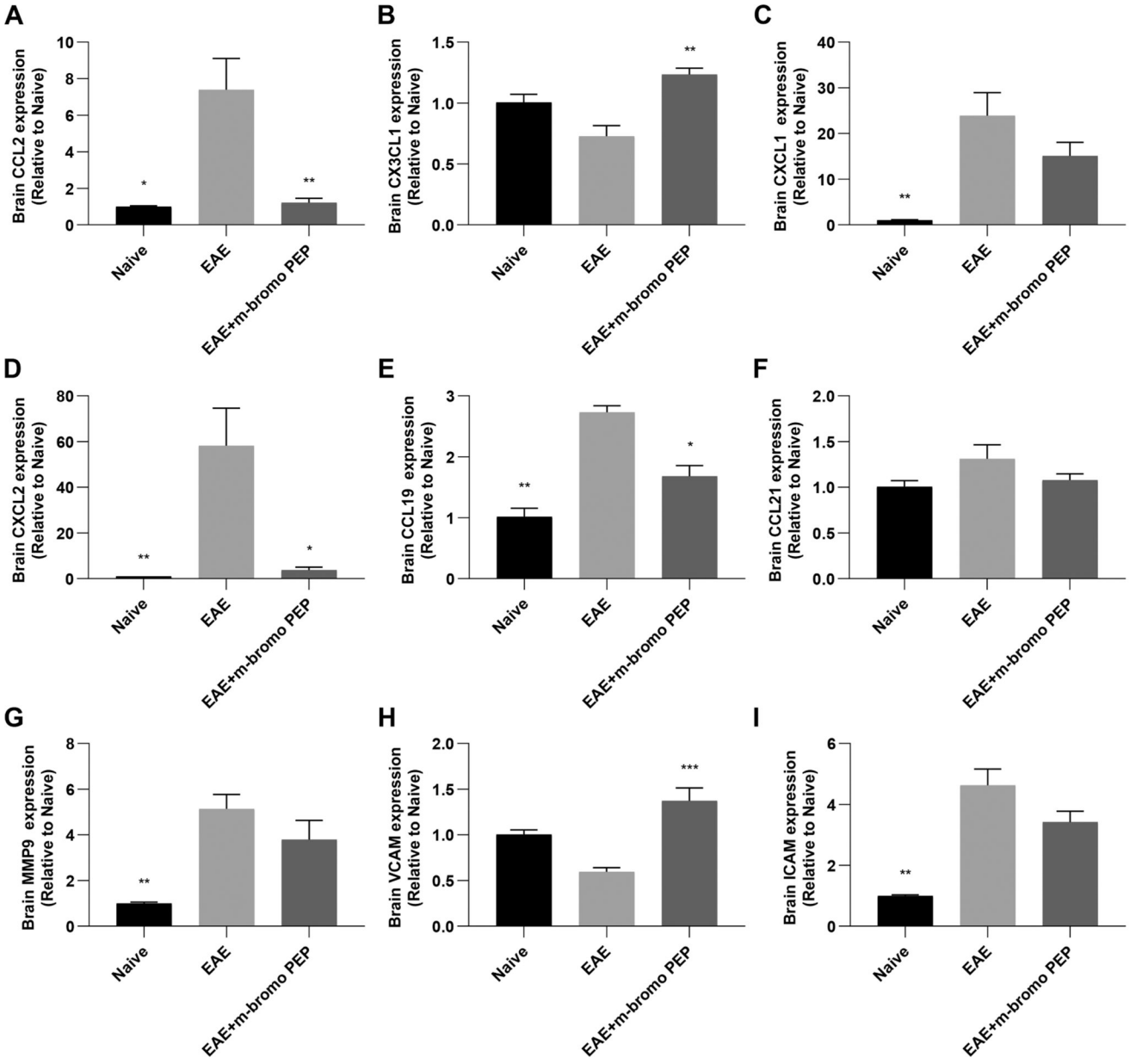

Fig. 7.

mRNA expression of genes important for immune cell infiltration into the CNS are inhibited by m-bromo PEP. Total RNA was purified from the brains of naive (n = 4), EAE (n = 7) and EAE + m-bromo PEP (n = 7) mice at day 16 post immunization, and mRNA expression of several immune cell recruitment genes were assessed by qRT-PCR. A-F, relative mRNA expression for the chemokines CCL2 (A), CX3CL1 (B), CXCL1 (C), CXCL2 (D), CCL19 (E) and CCL21 (F) are shown. G-I, The matrix metalloproteinase MMP-9 (G), and the adhesion molecules VCAM (H) and ICAM (I) are also depicted. Data are presented as mean ± SEM. *P < 0.05; **P < 0.01 vs EAE (Kruskal-Wallis one-way ANOVA, multiple comparisons with Dunn's correction).